DE GRUYTER

Nanotechnology Reviews 2022; 11: 770–792

Review Article

Jialin Liu, David Hui, and Denvid Lau*

# Two-dimensional nanomaterial-based polymer composites: Fundamentals and applications

https://doi.org/10.1515/ntrev-2022-0041
received September 10, 2021; accepted January 1, 2022

**Abstract:** Two-dimensional (2D) nanomaterial-reinforced polymer composites exhibit superior properties and multifunctional applications. Compared to lower dimensional nanomaterials such as nanotubes and nanoparticles, 2D nanomaterials show a larger surface area. The large surface area makes 2D nanomaterials more effectively restrict the mobility of polymer chains and yields better reinforcing efficiency than the lower-dimensional nanomaterials. To gain an in-depth understanding and extend the applications of polymer composites reinforced with 2D nanomaterials, this paper reviews the progress in the fundamentals of synthesis and applications of such composites. The motivation and improvement of adding 2D nanomaterials to polymer materials are introduced first, followed by the synthesis approaches and the properties of typical 2D nanomaterials, including graphene, boron nitride nanosheet, and molybdenum disulfide nanosheet. Based on the properties of 2D nanomaterials, polymer composites reinforced with different types of 2D nanomaterials are designed for structural application, thermal dissipation application, tribological application, three-dimensional printing composite structures, and strain sensing application. Afterwards, the significance of reinforcement–matrix interaction and its improving approach are reviewed. The current progress envisions that polymer composites reinforced with 2D nanomaterials can be used in the fields of aviation and aerospace for improving radiation shielding capacity and nanomedical engineering.

**Keywords:** nanosheets, interface, thermal dissipation, strain sensor, synthesis

## Abbreviations

| | |
|---|---|
| 2D | two-dimensional |
| 3D | three-dimensional |
| BNNS | boron nitride nanosheet |
| GO | graphene oxide |
| HPAM | hydrolyzed polyacrylamide |
| PEO | poly(ethylene oxide) |
| PET | polyethylene terephthalate |
| PLA | Polylactic acid |
| PMMA | polymethyl methacrylate |
| PS | polystyrene |
| PUB | polyurethane binder |
| PVA | polyvinyl alcohol |
| PVDF | poly(vinylidene fluoride) |
| rGO | reduced graphene oxide |
| SU-8 | epoxy-based photoresist |
| UHMWPE | ultra-high molecular weight polyethylene |

## 1 Introduction

Various types of nanomaterials have been used to modify the properties of polymer materials in previous research because pristine polymer materials lack high mechanical properties [1,2], thermal conductivity [3], and thermal stability [4]. Compared with conventional fibers, adding nanomaterials to polymer materials gives polymer composites better mechanical properties [5–7] and thermal and electrical conductivity [8,9]. Hence, polymer composites reinforced with nanomaterials have broad applications in practice such as military equipment [10,11], safety [12], protective clothing [12,13], automotive [14,15], aerospace [14–16], electronics [14,15,17], optical devices [14,16], medical devices [14], and constructions and buildings [18]. For a detailed discussion of the application of 2D nanomaterials for military equipment and protective

---

* **Corresponding author: Denvid Lau,** Department of Architecture and Civil Engineering, City University of Hong Kong, Hong Kong, China, e-mail: denvid.lau@cityu.edu.hk
**Jialin Liu:** Department of Architecture and Civil Engineering, City University of Hong Kong, Hong Kong, China
**David Hui:** Department of Mechanical Engineering, University of New Orleans, New Orleans, LA 70148, United States of America

clothing, the reader is advised to refer to a recent review article [19]. It is reported that the lower dimensional nanomaterials (*i.e.* nanotubes [20–24] and nanoparticles [25–28]) can improve the properties of the polymer. However, two-dimensional (2D) nanomaterials (*i.e.* nanosheets) exhibit a larger surface area than lower dimensional nanomaterials. The larger surface area provides more robust interfacial properties between 2D nanomaterials and polymer materials than those between lower dimensional nanomaterials and polymer materials. Therefore, 2D nanomaterials show a better reinforcing efficiency in properties of polymer materials than that of lower dimensional nanomaterials. For example, the thermal conductivity of pristine epoxy is increased by 133, 217, and 339% with the addition of 3 vol % (a volume fraction of 3%) boron nitride nanoparticles, boron nitride nanotubes, and boron nitride nanosheets (BNNS), respectively [29]. With the addition of 2D nanomaterials to polymer materials, the polymer composites show excellent performance and broad applications in practice.

The polymer composites exhibit advanced properties after curing owing to the admixture of 2D nanomaterials with polymer materials [30–34]. The mechanical properties [35–37], optical properties [38–40], thermal conductivity [41–43], electrical conductivity [37,44,45], and corrosion resistance [46,47] of polymer materials can be boosted by adding proper 2D nanomaterials. For example, with the addition of 0.3 wt% BNNS to polymethyl methacrylate (PMMA), the elastic modulus and the strength of PMMA are increased by 22 and 11%, respectively [35]. Besides, the transition temperature of PMMA is increased from 69 to 72°C [35]. The improvement made by 2D nanomaterials in the properties of polymer composites is dependent on the advanced physical properties of the 2D nanomaterials. 2D nanomaterials such as graphene and BNNS possess higher mechanical properties, thermal conductivity, and thermal stability than pristine polymer materials. Hence, it is expected that adding these 2D nanomaterials to polymer materials will improve the properties of polymer composites. However, the reinforcing efficiency of 2D nanomaterials in the properties of polymer composites is significantly dependent on the interfacial interaction between 2D nanomaterials and polymer materials. For example, the interface between BNNS and polymer materials accounts for the thermal conductivity of polymer composite [48]. Defects (*e.g.* voids and pores) at the reinforcement–matrix interface lead to ineffective thermal conduction in polymer composites [49,50]. To improve the interfacial interaction between 2D nanomaterials and polymer materials, the functionalization of 2D nanomaterials is adopted. The functionalized 2D nanomaterials present significant improvements in the properties of the polymer composites [34,51–57]. With the development of nanotechnology, various types of 2D nanomaterial-reinforced polymer composites are being designed and manufactured. These multifunctional polymer composites can be used in different fields. To utilize these polymer composites efficiently to meet the practical demands, it is of interest to specify their properties and applications.

This article aims to review the properties and applications of polymer composites reinforced with 2D nanomaterials. The applications of different types of 2D nanomaterial-reinforced polymer composites are summarized. We selected widely used 2D nanomaterials, such as graphene, BNNS, and molybdenum disulfide ($MoS_2$) nanosheet, as the typical materials. For these typical 2D nanomaterials, scalable synthesis is of great interest for practical application. Two types of synthesis approaches (*i.e.* the bottom-up approach and the top-down approach) were developed to produce the 2D nanomaterials. Based on these two approaches, different exfoliation techniques were used to prepare the nanomaterials on a large scale. Due to the development of synthesis techniques and the superior properties of 2D nanomaterials, 2D nanomaterials are widely used in practice for structural engineering, thermal dissipation, three-dimensional (3D) printing techniques, and strain sensing. In view of the fact that the interface between the reinforcement and matrix influences the properties of polymer composite reinforced with 2D nanomaterials, the significance of the reinforcement–matrix interaction is discussed. The effect of the functionalization of 2D nanomaterials on the improvement of the properties of the polymer composites is evaluated. The comprehensive knowledge of the fundamentals and the application of 2D nanomaterials in reinforcing polymer materials accelerates the development of reinforced composites. This development is of interest in terms of overcoming the shortcomings of the existing materials in engineering.

# 2 Fundamentals of the synthesis and physical properties of 2D nanomaterials

## 2.1 Synthesis of 2D nanomaterials

The synthesis of 2D nanomaterials can be divided into the bottom-up approach [58–61] and the top-down approach [62–65]. The bottom-up approach involves chemical/physical vapor deposition, molecular beam/atomic layer epitaxy, and chemical synthesis. This approach requires harsh reaction conditions and shows a low production rate in the fabrication of 2D nanomaterials [66–68]. The top-down approach involves chemical exfoliation and physical exfoliation. This approach is capable of producing scalable 2D nanomaterials in ambient conditions [67]. To have a comprehensive understanding of the synthesis approaches of 2D nanomaterials, a summary of different synthesis approaches is presented in Table 1. As the top-down approach is straightforward, cost-effective, and productive, this approach is widely used to fabricate 2D nanomaterials [69–71], which involves mechanical exfoliation, liquid-phase exfoliation, and electromechanical exfoliation.

Graphene is one of the most prevailing 2D nanomaterials; it was first synthesized by exfoliating oriented pyrolytic graphite in 2004 [78]. As exfoliation methods are productive and low cost, various types of exfoliation methods such as mechanical exfoliation [79,80], liquid-phase exfoliation [81,82], and electrochemical exfoliation [83–85] have been proposed to prepare graphene. The schematics of mechanical exfoliation are shown in Figure 1. The peel force in Figure 1(a) and shear force in Figure 1(b) are applied to the layer of graphene to overcome the van der Waals interaction between adjacent graphene [80,86]. As a result, the single layer of graphene is obtained by micromechanical cleavage [78,87,88] and balling milling methods [89,90]. The liquid-phase exfoliation is also an efficient way to synthesize 2D nanomaterials. For example, after the dispersion of graphite in organic solvents, the ultrasonication process is performed. The shear force induced by ultrasonication is applied to the bulk graphite. Due to the existence of cavitation in the bulk graphite, some voids in the bulk graphite are expanded under external shear force. As a result, graphene is exfoliated from bulk graphite [81,82]. Figure 2 shows the mechanism of electrochemical exfoliation for preparing graphene in the $(NH_4)_2SO_4$ aqueous solution [91]. By applying a constant bias voltage to the graphite electrodes, the water is reduced, creating hydroxyl ions in the electrolytes at the edge and the boundary of graphite, as shown in Figure 2(a) and (b). As a result, oxidation resulting from the attack of hydroxyl ions leads to expansion of the edge and boundaries of the graphite. This expansion allows $SO_4^{2-}$ anions and water molecules to penetrate into the adjacent layer in graphite, as shown in Figure 2(c). Furthermore, the oxidation of $SO_4^{2-}$ anions and water molecules yields gaseous products such as $SO_2$ and $O_2$ [92,93], which overcomes the weak van der Waals interaction between the adjacent graphene layers in the graphite. Therefore, graphene is exfoliated from bulk graphite by this electrochemical process, which is confirmed by experimental measures and observations [91].

**Table 1:** A summary of the bottom-up approach and top-down approach for synthesizing 2D nanomaterials

| Synthesis approaches | Bottom-up approach | | | Top-down approach | |
|---|---|---|---|---|---|
| | Chemical/physical vapor deposition | Molecular beam/atomic layer epitaxy | Chemical synthesis | Chemical exfoliation | Physical exfoliation |
| Advantages | (a) The resolution of nanosheets can be controlled to distinguish the angstrom-level difference [72]<br>(b) The stacking number of nanosheets can be controlled by the bottom-up approach [73] | | | (a) The top-down approach is able to address the precise locations and sizes of nanosheets [74]<br>(b) The top-down approach is simple, straightforward, and cost-effective [69–71] | |
| Limitations | (a) The bottom-up approach is slow, laborious, and expensive owing to the requirements of aggressive reaction conditions (*e.g.* high energy, reduced atmosphere, and long reaction period) [74,75]<br>(b) It is less precise to place nanosheets prepared by the top-down approach in the expected location [76] | | | (a) The sizes of nanosheets prepared by the top-down approach are limited by the size of the starting materials [75]<br>(b) The stabilization of nanosheets prepared by the top-down approach is low, resulting in restacking of nanosheets [73,77] | |

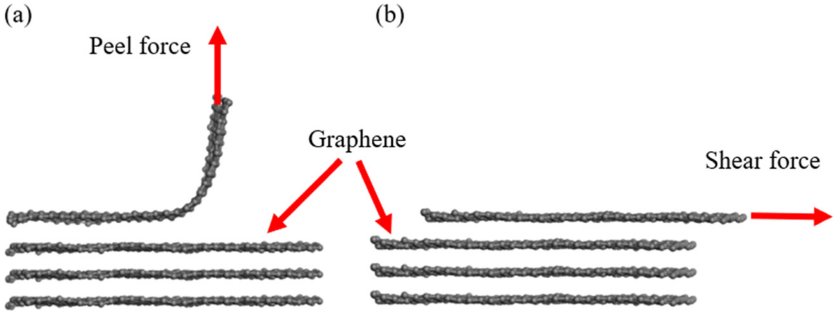

**Figure 1:** Schematics of mechanical exfoliation to obtain a single layer of graphene by applying (a) peel force and (b) shear force.

BNNS, as an analog of graphene, is termed "white graphene" because of its white appearance [94]. The available exfoliation methods for preparing BNNS are mechanical exfoliation, liquid-phase exfoliation, and electrochemical exfoliation. The first isolation of BNNS was exfoliated by mechanical cleavage in 2008 [95]. Following this, different types of mechanical exfoliation techniques were developed. Figure 3 shows the mechanisms of exfoliating BNNS by ball milling [96]. Ball milling is a shear force-dominant process used to exfoliate BNNS from bulk boron nitride materials. When the metallic balls, grinding media, and bulk boron nitride materials are placed in the rotating shell, the bulk boron nitride materials are splintered by the shear force and peel force created by the metallic rotating balls [97,98]. As a result, the van der Waals interaction between adjacent BNNS in bulk boron nitride materials is overcome, which yields one-atom-thick BNNS. To avoid damage to the structure of BNNS, the exfoliation method is improved by adopting controllable balling, small milling media, and appropriate milling media types as lubrication during the milling process [99]. In addition, atomic force microscope tips are employed to delaminate the multilayers of boron nitride flakes based on mechanical exfoliation. Furthermore, a mechanochemically delaminated method and ion intercalation–assisted electrochemical exfoliation are used to prepare BNNS.

Transition metal dichalcogenide nanosheets, including $MoS_2$ nanosheet and tungsten disulfide nanosheet, can also be synthesized by mechanical exfoliation. However, as mechanical exfoliation uses a decent microscope and adhesive tape to prepare nanosheets, it cannot produce 2D nanomaterials on a large scale [100]. The liquid-phase exfoliation method, in contrast, can be used to produce 2D nanomaterials on a large scale; however, this exfoliation method shows

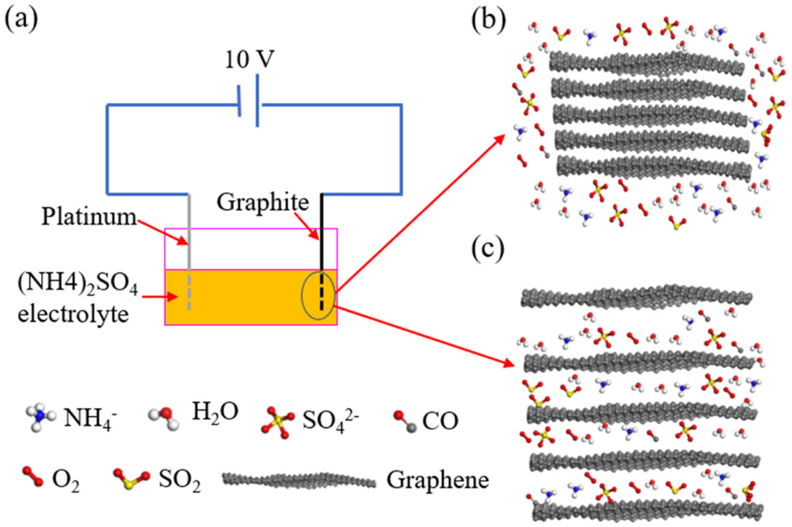

**Figure 2:** Electrochemical exfoliation of graphene in $(NH_4)_2SO_4$ aqueous solution. (a) The bias voltage is applied on the graphite electrodes in the $(NH_4)_2SO_4$ aqueous solution. (b) The attack of ions results in the expansion of graphite on the edge and boundary, which allows $SO_4^{2-}$ anions, water molecules, and gas to penetrate into the adjacent layer in graphite. (c) The penetration of ions, water molecules, and gas in graphite overcomes van der Waals interaction between interlayers of graphite, which yields graphene.

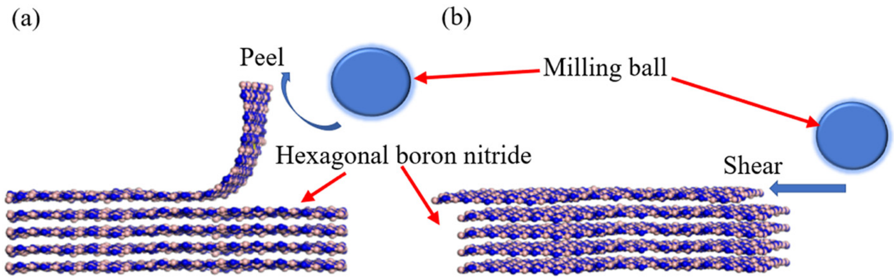

**Figure 3:** Schematics of exfoliating BNNS from hexagonal boron nitride under (a) peel force and (b) shear force created by the metallic balls in the rotating shell.

a significant overlap in the transition metal dichalcogenide flakes and the in-plane resistance of transition metal dichalcogenide film [100,101]. Hence, neither mechanical exfoliation nor liquid-phase exfoliation is widely used for the synthesis of transition metal dichalcogenide nanosheets. Instead, the molecular beam epitaxy, chemical vapor deposition, and chemical vapor deposition-related methods are used to prepare transition metal dichalcogenide nanosheets. Chemical vapor deposition is one of the most practical methods for synthesizing transition metal dichalcogenide nanosheets such as molybdenum disulfide ($MoS_2$) nanosheets [100,102]. In contrast to molecular beam epitaxy, the ultrahigh vacuum chamber is not required in chemical vapor deposition. Hence, the chemical vapor deposition is cheap and compatible with the existing synthesis process [100,103]. The first report on synthesis based on chemical vapor deposition yielded multilayers of $MoS_2$ nanosheet [104]. To control the thickness of the $MoS_2$ nanosheet, chemical vapor deposition using sulfur and molybdenum oxide powders is used to yield the growth of the $MoS_2$ nanosheet on the $SiO_2$ substrate [105,106]. The principle for synthesizing $MoS_2$ nanosheet using chemical vapor deposition is presented in Figure 4. Before the synthesis of the $MoS_2$ nanosheet, the reduced graphene oxide (rGO) solution is spined on the surface of the $SiO_2$ substrate, as shown in Figure 4(a). Subsequently, the $SiO_2$ substrate with rGO solution is dried in a furnace at 50°C, as shown in Figure 4(b). The $SiO_2$ substrate is then placed in a furnace with sulfur (S) powder and molybdenum oxide ($MoO_3$) powder at 650°C in a nitrogen environment, as shown in Figure 4(c). In Figure 4(c), the S powder and $MoO_3$ powder are placed in two separate ceramic vessels. At the temperature of 650°C, the S vapor is carried by the nitrogen gas to react with the $MoO_3$ powder, yielding volatile suboxide $MoO_{3-x}$ compound. $SiO_2$ substrate is placed on top of the ceramic vessel with the $MoO_3$ powder and faced with the $MoO_3$ powder. Hence, the volatile suboxide $MoO_{3-x}$ compound can react with the S vapor on the surface of the $SiO_2$ substrate. As a result, the reaction product (*i.e.* $MoS_2$ film) grows on the surface of the $SiO_2$ substrate.

## 2.2 Structures and properties of 2D nanomaterials

The structures and properties of typical 2D nanomaterials are significantly different, which results in different applications of polymer composites reinforced with 2D nanomaterials.

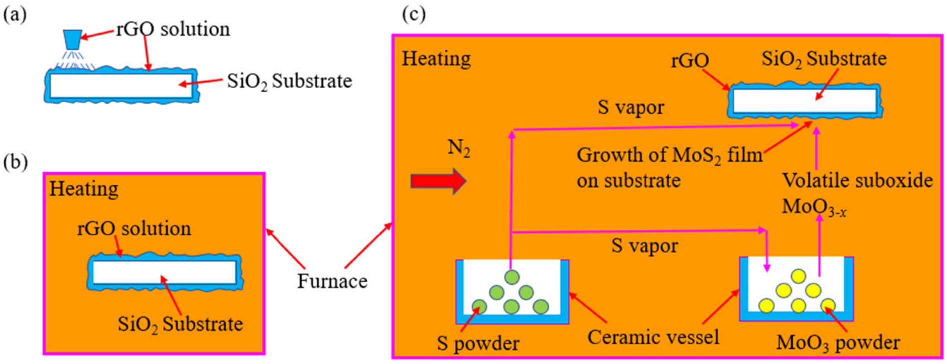

**Figure 4:** The principle of chemical vapor deposition for synthesizing $MoS_2$ nanosheet based on the reaction between sulfur (S) and molybdenum oxide ($MoO_3$) at elevated temperature. (a) The rGO solution is spun on the surface of the $SiO_2$ substrate. (b) The rGO solution is dried in a furnace at 50°C. (c) The sulfur (S) powder and molybdenum oxide ($MoO_3$) powder are put in a furnace at 650°C in a nitrogen environment.

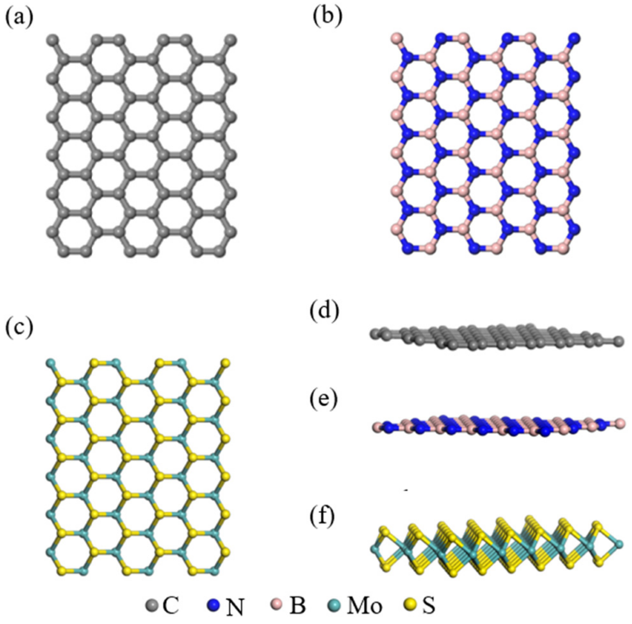

**Figure 5:** The in-plane structures of (a) graphene, (b) BNNS, and (c) $MoS_2$ nanosheet, and the lateral structure of (d) graphene, (e) BNNS, and (f) $MoS_2$ nanosheet.

Figure 5 shows the in-plane structure and lateral structure of graphene, BNNS, and $MoS_2$ nanosheet. Graphene is structurally similar to BNNS, as shown in Figure 5(a)–(d), and the boron–nitrogen bonds in BNNS are polarized, offering a partial ionicity [107]. Hence, the boron atoms and nitrogen atoms are partially charged. The partially charged atoms in BNNS exhibit electrostatic interaction with polymer materials, while the carbon atoms in graphene exhibit no partial ionicity. The presence of van der Waals interaction and electrostatic interaction between BNNS and polymer materials is advantageous as it allows the BNNS to form robust interfacial interaction with the polymer materials [33]. As a result, BNNS shows more robust interaction with polymer materials than graphene [108]. Besides, for the multilayered BNNSs, the interlayer interaction between adjacent BNNSs differs from graphene. It is reported that the interlayer shear modulus and bending rigidity of multilayered BNNSs are approximately three times as large as those of graphene, which is attributed to the robust interlayer interaction between polarized boron and nitrogen atoms restricting the interlayer shear sliding of multilayered BNNSs [109,110]. For $MoS_2$ nanosheet, its in-plane structure is similar to that of BNNS and graphene. However, the lateral structure of $MoS_2$ nanosheet is totally different from BNNS and graphene. BNNS and graphene possess flat planes in the lateral view, while $MoS_2$ nanosheet presents a sandwich structure in the lateral view, as shown in Figure 5(d)–(f). The Mo-atom layer is sandwiched by two S-atom layers forming the weak sandwich structure [111]. The S–Mo–S sandwich structure is assembled due to van der Waals interaction. The weak interlayer interaction between sandwich structures results in relative sliding between the layers [111,112].

The physical properties of graphene, BNNS, and $MoS_2$ nanosheets are different, as presented in Table 2. These three types of 2D nanomaterials show excellent thermal stability, as indicated by the oxidation resistance in Table 2. Young's modulus of graphene and BNNS are comparable; they are larger than that of $MoS_2$ nanosheet. However, Young's modulus and tensile strength of $MoS_2$ nanosheet are still much higher than those of conventional materials (*e.g.* steel). The thermal conductivity of graphene is superior, as presented in Table 2. Hence, graphene is a good candidate for improving the thermal dissipation of polymer materials. However, the bandgap of graphene is close to zero, indicating that it is electrically conductive. Hence, graphene cannot be used in the thermal dissipation of electronics, where dielectricity of reinforcement is required. Instead, BNNS with a high value of bandgap indicates its insulating characteristic. In addition, the bandgap of $MoS_2$ is tunable under mechanical strain. Hence, the electrical conductivity of $MoS_2$ nanosheet can be modulated due to the changing strain of the nanosheet [113]. $MoS_2$ nanosheet's coupling of electrical conductivity with mechanical properties provides the potential for developing a polymer composite sensor reinforced with this nanosheet.

# 3 Applications of polymer composites reinforced by 2D nanomaterials

## 3.1 Structural application

2D nanomaterials (*e.g.* graphene [119,120], BNNS [121], and $MoS_2$ nanosheet [122,123]) exhibit excellent tensile strength and Young's modulus. With the addition of BNNS to polymer materials, it is expected that the tensile strength and Young's modulus of polymer materials can be significantly improved. The simple estimation of Young's modulus of 2D nanomaterial-reinforced polymer composites is shown in equation (1).

$$E_C = E_M V_M + E_R V_R, \tag{1}$$

where $E_C$ is Young's modulus of the polymer composite, $E_m$ is Young's modulus of the matrix, $E_f$ is Young's modulus of reinforcement, $V_m$ is the volume fraction of the matrix, and $V_R = 1 - V_M$ is the volume fraction of the

**Table 2:** Properties of graphene, BNNS, and $MoS_2$ nanosheet

| **Properties** | **Graphene** [114] | **BNNS** [114] | **$MoS_2$ nanosheet** [115–118] |
|---|---|---|---|
| Oxidation temperature in air (°C) | ~600 | ~840 | ~1,100 |
| Young's modulus (TPa) | 1.1 | 0.81–1.3 | 0.26–0.4 |
| Thermal conductivity ($W\,m^{-1}\,K^{-1}$) | 2,600 | 400 | ~52 |
| Bandgap (eV) | ~0 | 5.5–6.0 | 1.8 |

nanofiller. This simple model for estimating Young's modulus can be used to determine the upper bound of Young's modulus of a polymer composite reinforced with 2D nanomaterials. The lower bound of Young's modulus of a polymer composite reinforced with 2D nanomaterials is calculated by equation (2).

$$E_C = \frac{E_M E_R}{E_M V_M + E_R V_R}. \qquad (2)$$

The excellent reinforcing efficiency of 2D nanomaterials in the static mechanical properties of polymer materials, as shown in Table 3. Specifically, with the addition of 2D nanomaterials, the improvement of Young's modulus and tensile strength of polymer materials are in the range of 14–71 and 11–130%, respectively. For PVA, the addition of graphene shows better reinforcing efficiency in Young's modulus than that of BNNS and $MoS_2$ nanosheet, while the addition of $MoS_2$ nanosheet to polymers shows better reinforcing efficiency in tensile strength than that of graphene and BNNS. The improvement of Young's modulus of the polymer composites is attributed to the intrinsic superior Young's modulus of these 2D nanomaterials. With the addition of a reinforcement that has a higher Young's modulus than that of the matrix, the polymer composites gain a higher Young's modulus than that of the matrix materials. The tensile strength of polymer composites reinforced with 2D nanomaterials is attributed to the efficient stress transfer at the reinforcement–matrix interface [129]. Specifically, nanosheet adsorbs polymer chains and restricts the motion of polymer chains due to the interfacial interaction between nanosheets and polymer materials [130]. Therefore, the tensile strength of polymer composite reinforced with 2D nanomaterials is significantly improved. Furthermore, adding nanosheets to polymer materials reduces the formation of microscale voids in polymer materials. Voids in polymer materials evolve into defects under tension, which weakens the tensile strength of pristine polymer materials [131]. However, adding 2D nanomaterials to polymer materials yields densified structures. It is reported that there are microscale voids in pristine poly(ethylene oxide) (PEO), whereas there is no visible microscale void in PEO reinforced with $MoS_2$ nanosheet under the same magnification. The experimental observation indicates that adding $MoS_2$ nanosheet to PEO refines the microstructure and reduces the defects in PEO composites [132]. The scanning electron microscope figures are provided in ref. [132]. As a result, the tensile strength of the polymer composite is significantly improved. While the reinforcing efficiency of 2D nanomaterials in static mechanical properties of polymer composites is very good, the reinforcing efficiency of 2D nanomaterials in the dynamic properties of polymer composites is not studied in the aforementioned research. The dynamic properties of polymer composite are very important because the resistance of polymer composite to dynamic loads exhibits good durability and impact protection in case of a car crash, bird striking of the plane, ship collision, *etc.* Hence, the dynamic properties of 2D nanomaterial-reinforced polymer composites are reviewed.

2D nanomaterials are added to fiber-reinforced polymer composites for improving the dynamics properties of polymer composites [133,134]. The fiber-reinforced polymer composite is widely used in automobiles, planes, ship structures, *etc.*,

**Table 3:** Mechanical improvement of polymer materials reinforced by typical 2D nanomaterials

| **Polymer materials** | **2D nanomaterials (weight fraction)** | **Young's modulus (improvement)** | **Tensile strength (improvement)** |
|---|---|---|---|
| Epoxy [124] | Graphene (2%) | 2 GPa (58%) | 55 MPa (130%) |
| UHMWPE [125] | Graphene (1%) | 1.24 GPa (44%) | 22.2 MPa (76%) |
| PMMA [35] | BNNS (0.3%) | 2.13 GPa (22%) | ~42 MPa (11%) |
| PVA [126] | Graphene (0.4%) | 8.2 GPa (71%) | 110 MPa (16%) |
| PVA [127] | BNNS (0.8%) | 2.69 GPa (17%) | 91 MPa (18%) |
| PVA [128] | $MoS_2$ nanosheet (0.25%) | 3.2 GPa (14%) | 127 MPa (18%) |

due to its lightweight characteristic and high mechanical performance [135,136]. However, the fiber-reinforced polymer composites (*e.g.* carbon fiber-reinforced epoxy composite) show brittle nature. As a result, the carbon fiber-reinforced epoxy composite, for example, shows a sharp drop in stress–strain curves with low-energy absorption capacity [137]. This brittleness of polymer composite decreases impact protection of polymer composite structures in case of the aforementioned car crash, bird striking of the plane, ship collision, *etc.* 2D nanomaterial-reinforced polymer composite exhibits excellent fracture toughness [137,138], which makes 2D nanomaterials attractive candidates for improving the impact resistance of fiber-reinforced polymer composites. It is reported that the mode II interlaminar fracture toughness of carbon fiber-reinforced epoxy composite is increased by 46.7% with the addition of 2% (weight fraction) nanosheets owing to the crack deflection when the cracks encounter the nanosheets [139]. With the improvement of 2D nanomaterials in the fracture toughness of polymer composite, the impact protection of composite structures made of carbon fiber-reinforced polymer composites can be significantly increased. The picture of 2D nanomaterial-reinforced polymer composite structures is shown in Figure 17 in ref. [140].

## 3.2 Thermal dissipation

The development of miniaturization has required high thermal dissipation of various products (*e.g.* the battery units in electric vehicles and central processing units in smartphones and tablets) in the pursuit of high performance, reliability, longevity, and safety [141–143]. However, the materials used for thermal transport in electric vehicles and smartphones exhibit low thermal conductivity. The thermal conductivity of most polymer materials ranges from 0.1 to 0.5 $\mathrm{W\,m^{-1}\,K^{-1}}$ [144]. Various types of 2D nanomaterials show the potential to improve the thermal transport of polymer materials, owing to their superior thermal conductivity and thermal stability [145–147]. Furthermore, 2D nanomaterials form efficient heat-conducting paths across polymer materials at low volume fractions due to the large surface area of the 2D nanomaterials [148]. One typical example is graphene, which has superior thermal conductivity and thermal stability, as presented in Table 2. It is worth noting that graphene presents a zero value at the bandgap, indicating that it is an excellent electric conductor. Adding excellent electric conductors such as graphene to polymer materials can increase the electrical conductivity of polymer composites. Hence, graphene-reinforced polymer composites are unsuitable to be used in electronics, as it is necessary to avoid short circuits. However, BNNS displays electrical insulation, thermal stability, and good thermal conductivity [149]. Hence, it is a perfect candidate for improving thermal transport in electronics and electric vehicles.

The thermal transport of polymer composites reinforced with 2D nanomaterials has been studied in previous studies [150,151]. The picture of 2D nanomaterial-reinforced polymer composite products for thermal management is shown in Figure 5 in ref. [152]. It is reported that the conductivity of epoxy is increased from ~0.2 to ~1.5 $\mathrm{W\,m^{-1}\,K^{-1}}$ by adding graphene at a proportion of 2.8 vol% [150]. The thermal conductivity of these polymer composites is significantly dependent on the polymer materials due to the high content of these polymer materials in the composites. As a result, the thermal conductivity of epoxy composite reinforced with graphene is still much lower than that of graphene with thermal conductivity of 2,600 $\mathrm{W\,m^{-1}\,K^{-1}}$. To take advantage of the thermal conductivity of 2D nanomaterials, the proportion of 2D nanomaterials should be increased. By increasing the amount of 2D nanomaterials in polymer composites, the thermal conductivity of polymer composites will be significantly increased. For example, the in-plane thermal conductivity of BNNS-reinforced poly(diallyl dimethyl ammonium chloride) is increased from ~0 to 220 $\mathrm{W\,m^{-1}\,K^{-1}}$ when the proportion of BNNS content is increased from 0 to 90% [152]. In the existing literature, it is reported that the ordered alignments of reinforcement in polymer significantly optimize the heat transfer from the 2D nanopaper to shape memory polymer resin [153]. For further improvement of the thermal conductivity of polymer composites, BNNSs, for example, are aligned to form linear densely packed boron nitride structures in polymer materials, as shown in Figure 6. The linear densely packed boron nitride structure–reinforced polymer composite transports the heat in the polymer materials through the thermal conduction routes. However, the thermal dissipation of 2D nanomaterial-reinforced polymer composites has some limitations. The limitations of two-dimensional nanomaterials in thermal dissipation include the anisotropic thermal conductivity, the interfacial thermal resistance, and the interfacial phonon scattering induced by defects and mismatches at the reinforcement–matrix interface. While the linear densely packed boron nitride structures in the polymer can effectively increase the thermal transport along the thermal conduction routes, as shown in Figure 6, the thermal conductivity in the direction of perpendicular to the thermal conduction routes is still very low. It is expected that a network structure can be inserted

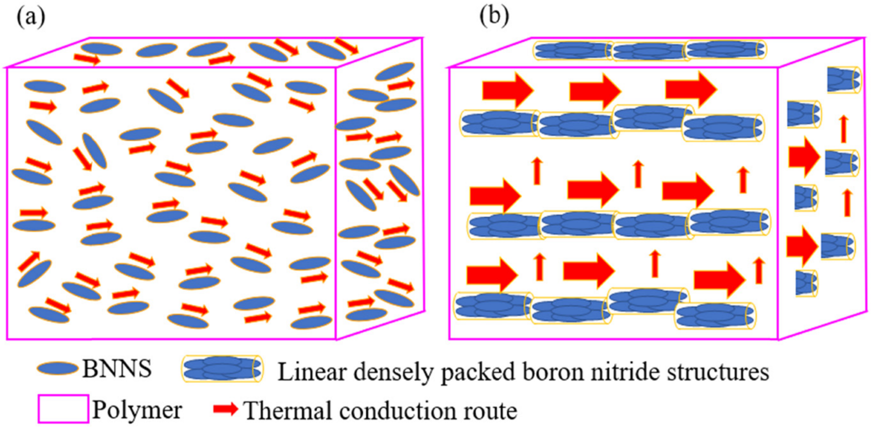

**Figure 6:** Schematic illustrations of thermal conduction routes in polymer composites reinforced by (a) randomly distributed BNNS and (b) oriented linear densely packed BN structure. The larger arrows indicate that the thermal conduction is more efficient than that of the smaller arrows.

into polymer composite so that the thermal conductivity of polymer composite is significantly increased in different directions. Besides, the efficient thermal conduction at the interface between two-dimensional nanomaterials and polymer restricts the improvement of two-dimensional nanomaterials in the thermal conductivity of polymer composite. It is reported that an abrupt temperature drop occurs across the interface between graphene and PMMA [154], indicating inefficient thermal transport across the reinforcement–matrix interface. This inefficient thermal transport is mainly due to the interfacial thermal resistance between graphene and PMMA, which significantly decreases the improvement in the thermal conductivity of polymer composites reinforced with 2D nanomaterials. Furthermore, the weak interfacial interaction between 2D nanomaterials and polymer materials leads to defects and mismatches at the reinforcement–matrix interface. The defects and mismatch act as the phonon scattering decrease the thermal conductivity of polymer composites [33,155,156]. This limitation can be solved by improving the interfacial interaction between two-dimensional nanomaterials and polymer through the functionalization of 2D nanomaterials.

## 3.3 Tribological application

Polymer materials such as epoxy are widely used in automobile, aerospace, marine, *etc.* [157]. It is not uncommon that the contact between two moving surfaces of structures in engineering leads to friction and wear of polymer materials, which results in friction heat build-up due to the high sliding between contacted surfaces and structural damage in the structures [158,159]. To reduce the friction heat and avoid structural damage, it is necessary to mitigate the coefficient of friction and improve the thermal conductivity and the mechanical properties of polymer composites [160,161]. 2D nanomaterials exhibit high mechanical properties, thermal conductivity, and low friction, making 2D nanomaterials an attractive solid lubricant. The picture of 2D nanomaterial working as a lubricant for machine element is provided in Figure 1 in ref. [162]. In the existing literature, it is reported that the addition of 2 wt% BNNS to polyimide and the addition of 0.5 wt% BNNS to epoxy reduce the wear rate of polymer composites by 83 and 33%, respectively [163,164]. The addition of 0.5 wt% BNNS to epoxy shows a 17% reduction in the coefficient of friction [163]. Compared to the fiber reinforcement (*e.g.* glass fiber) and particle reinforcement (*e.g.* silicon carbide particles), 2D nanosheets possess lower density than the fiber reinforcement and particle reinforcement [165]. As a result, 2D nanosheets can be well dispersed in polymer composites. Besides, 2D nanomaterials show better compatibility with polymer materials than that of fiber reinforcement and particle reinforcement [159]. Hence, the stress transfer and thermal conduction at the interface between 2D nanomaterials and polymer materials are efficient, which significantly improves the mechanical properties and thermal conductivity of polymer composites. Unlike one-dimensional nanomaterials (*e.g.* carbon nanotubes (CNTs) and boron nitride nanotubes), multilayered 2D nanomaterials due to agglomeration show weak van der Waals interaction between adjacent layers. As a result, the shear sliding between interlayers of 2D nanomaterials occurs easily. The easy shear sliding between the large smooth surfaces of multilayered 2D nanomaterials exhibits the self-lubricant characteristic, which is beneficial to reduce the coefficient of friction of polymer composites [166,167]. The low coefficient of friction of polymer composites can reduce the build-up of the friction heat and the frictional force, which is of interest to avoid structural damage. Hence, 2D nanomaterials are very attractive to improve the tribological performance of polymer composites.

2D nanomaterials working as solid lubricants for improving the tribological performance of polymer materials are desirable to be highly durable, easy to deliver to the contact interfaces, and environmentally insensitive [166]. Graphene, BNNS, and $MoS_2$ nanosheets are highly durable 2D nanomaterials under thermal conditions and loadings because of their high thermal stability and mechanical properties, as shown in Table 2, and chemical inertness. The durability of 2D nanomaterials is helpful to maintain the tribological performance of 2D nanomaterial-reinforced polymer composites. Due to the good dispersion and ultrathin shape of 2D nanomaterials in polymer composites, 2D nanomaterials can easily enter the contact area of sliding surfaces [168]. However, the friction and wear of graphene, BNNS, and $MoS_2$ nanosheet are influenced by environmental humidity. It is reported that the friction and wear of graphene decrease when the environmental humidity increases [169,170]. The reduction of friction and wear of graphene in high environmental humidity is attributed to the repair of the bond broken area. Specifically, water molecules disassociate and yield hydrogen radicals and hydroxyl radicals. These radicals react with the carbon dangling bonds and repair the damaged graphene [170]. As a result, graphene maintains its function as a lubricant. BNNS shows similar dependence on the environmental humidity to graphene [171]. However, the friction and wear of $MoS_2$ nanosheet increases when the environmental humidity increases. The rising of friction and wear of $MoS_2$ nanosheet is due to the accelerated oxidation on the surface of $MoS_2$ nanosheet in water molecules. Besides, the occupation of the wedge-shaped cavities of $MoS_2$ nanosheet increases the adhesion force on the sliding surfaces [171]. Hence, graphene and BNNS are proper candidates for improving the tribological performance of polymer composites in humid environments, while $MoS_2$ nanosheet is a proper candidate for improving the tribological performance of polymer composites as a dry lubricant.

## 3.4 Three-dimensional printed composites

The 3D printing technique is a promising method for preparing composite structures owing to its reliability, automated construction, simple fabrication, and low cost [172–175]. To maintain the shape stability of 3D-printed polymer composites and avoid their collapse, 2D nanomaterials (*e.g.* graphene) are added to improve the viscosity of polymer composites. When 2D nanomaterials are added to polymer materials, a robust interfacial interaction between 2D nanomaterials and polymer materials forms. The motion of polymer chains is restricted by 2D nanomaterials. As a result, the viscosity of polymer materials is increased by adding 2D nanomaterials [176]. Concurrently, these composites show a shear-thinning behavior. The shear-shinning behavior means that the viscosity of composites decreases with the increasing shear rate. It is reported that hydrolyzed polyacrylamide (HPAM) reinforced by graphene-based nanosheet shows a lower viscosity than the initial viscosity of pristine HPAM when the shear rate is increased [176]. Due to the reduced viscosity of polymer composites at a high shear rate, the polymer composites reinforced with 2D nanomaterials assure a smooth printing process during its flow in the extrusion nozzle. Furthermore, the viscosity of polymer composites can be reduced by heating the print head and the nozzle plate [176,177]. In addition to the printability and shape stability of 3D-printed polymer composites, adding 2D nanomaterials to polymer materials can also improve the mechanical and thermal conductivity of 3D-printed composite structures, as mentioned in Secs. 3.1 and 3.2, respectively. The picture of 3D-printed mechanical gear with 2D nanomaterial-reinforced PLA is provided in Figure 1 in ref. [178].

3D-printed polymer composite can prepare oriented 2D nanomaterials in polymer materials [178,179]. The oriented 2D nanomaterials create a thermal conduction route for thermal dissipation in polymer composite. Based on the extrusion method, the 2D nanomaterials are aligned along the printing direction [180]. The 2D nanomaterials are oriented due to the shear force in the printing process, which aligns the 2D nanomaterials along the same direction, as presented in Figure 7 [178]. First, GO solution is sprayed on the surface of the glass substrate to form a GO membrane, as shown in Figure 7(a). Subsequently, PLA solution is cast onto the GO membrane to obtain PLA/GO membrane, as shown in Figure 7(b). Following this, the PLA/GO membrane is peeled off from the glass substrate and scrolled to obtain the scrolled PLA/GO membrane, as shown in Figure 7(c) and (d). The interface between GO and PLA membranes is strong due to the hydrogen bond interaction between them, which ensures that the GO/PLA membrane can be peeled off from the glass substrate smoothly without deteriorating the GO/PLA interface. Finally, the scrolled PLA/GO membrane is added to the PLA to be printed using the 3D printing technique, which yields the oriented PLA/GO membrane in 3D-printed composite.

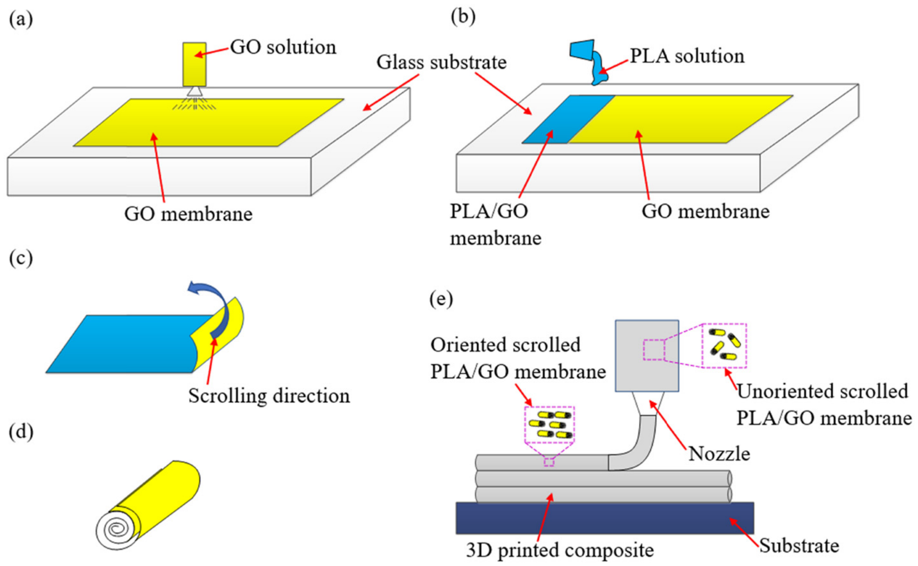

**Figure 7:** Schematic diagram of making highly oriented 2D nanomaterials for 3D printed composites. (a) Graphene oxide (GO) solution is sprayed on the surface of the glass substrate to form a GO membrane. (b) Polylactic acid (PLA) solution is cast on the surface of GO solution to form PLA/GO membrane. (c) PLA/GO membrane is scrolled. (d) Unoriented scrolled PLA/GO membrane is transferred to oriented scrolled PLA/GO membrane in 3D printed composite. (e) 2D nanomaterials are oriented in the 3D printed structures.

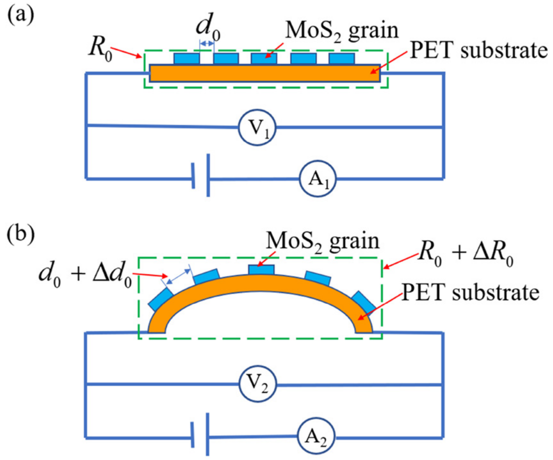

**Figure 8:** Schematics of measuring the current–voltage curves of $MoS_2$ film/PET composite sensor at (a) relaxed state and (b) stressed state. $d_0$ and $d_0 + \Delta d_0$ are the tunneling gap between $MoS_2$ films at the relaxed and stressed states, respectively. $R_0$ and $R_0 + \Delta R_0$ are the resistance of the $MoS_2$ film/PET composite at relaxed and stressed states, respectively.

## 3.5 Strain sensor application

A strain sensor is a widely used sensor that identifies and responds to mechanical motion, exchanging this motion with an electrical signal based on the electrical resistance of polymer materials [181]. However, the low sensitivity of polymer materials to small mechanical strain restricts the applications of strain sensors [182,183]. 2D nanomaterials are attractive candidates for improving the sensitivity to applied strain and the functionality of polymer sensors. The sensitivity of the strain sensor is defined as the gauge factor. It is reported that the graphene-based thermoplastic polyurethane shows a gauge factor of 35.7 at the applied strain higher than 60% [184]. This value is much higher than that of carbon nanotube-based thermoplastic polyurethane. It is reported that carbon nanotube-based thermoplastic polyurethane shows a gauge factor of 7.08 at the applied strain of 100% [185]. Figure 8 shows the process of making $MoS_2$ nanosheet-reinforced polymer composite sensor and the electrical response of the composite strain sensor to the mechanical deformation. First, the gold electrodes are deposited on the flexible substrate, which is made of polyethylene terephthalate (PET). The $MoS_2$ nanosheet is then encapsulated by SU-8 (epoxy-based photoresist) polymer to obtain the composite sensor. The composite sensor is stressed due to bending deformation, which increases the tunneling gap in the $MoS_2$ grain (made of nanosheet-reinforced polymer) from $d_0$ to $d_0 + \Delta d_0$, as shown in Figure 7(a) and (b). As a result, the potential barrier for electrons passing through the tunneling gap is increased, which suppresses the current, indicating that the resistance of the composite sensor is increased from $R_0$ to $R_0 + \Delta R_0$. The relationship between the average tunneling gap and the resistance is determined by the tunneling and destruction model [186,187], which is calculated by equations (3) and (4).

$$R = \frac{8\pi hL}{3A^2XdD}e^{Xd}, \tag{3}$$

$$X = \frac{4\pi(2m\phi)^{1/2}}{h}, \tag{4}$$

where $R$ is the resistance between grains, $h$ is the plank's constant, $L$ is the grain number, $A$ is the effective area of the grain, $d$ is the average tunneling gap between grains, $D$ is the number of the current path through the grains, $m$ is the mass of an electron passing through the tunneling gap, and $\phi$ is the potential barrier between adjacent grains [188]. The resistance of the composite sensor can be quantified based on the measurements of the current and voltage at different levels of stress. The results indicate that composite reinforced with $MoS_2$ nanosheet exhibits outstanding piezoresistive properties, which couple electrical properties with mechanical properties. Moreover, when 2D nanomaterials are added to polymer materials, the composite sensor shows better durability due to improved mechanical properties. It is reported that the polymer composite remains intact even under a high-stress level beyond 14 MPa due to the improvement of the 2D nanomaterial in the mechanical properties of $MoS_2$-reinforced SU-8 polymer composite [188].

In addition to the strain sensor made of $MoS_2$-based polymer composite, there are strain sensors made by BNNS-based polymer composites [184] and graphene-based polymer composites [189,190]. For example, it is reported that a self-powered strain sensor made of graphene-based ecoflex composite film is obtained due to the thermal gradient between human skin and the ambient environment, which can bear 1,000 cycles of repetitive strains and show a strain resolution of 0.125% with response time in 0.6 s [191]. Figure 9 shows the schematic of the self-powered thermoelectric device made of graphene-based ecoflex composite. When the heater and cooler are applied on the heating side and cooling side, respectively, the thermal gradient ($\Delta T = T_1 - T_2$) across graphene-based ecoflex composite film is obtained. As a result, the graphene-based ecoflex composite film yields voltage and current due to the thermal gradient between human skin and the ambient environment. Specifically, under the thermal gradient of $\Delta T = 14.5$ K, the graphene-based ecoflex composite film yields direct current output with the voltage of ~0.48 mV and the current of ~130 nA [191]. In view that the voltage yielded by the self-powered thermoelectric device is dependent on the thermal gradients between human skin and the ambient environment and is independent of the level of the strain of the graphene-based ecoflex composite film, the level of the strain of the graphene-based ecoflex composite film can be related to the current yielded by the self-powered thermoelectric device under a certain thermal gradient. The measurements show that the current yielded by the thermoelectric device is decreased as the strain of the composite film is increased under external loading because the electrical resistance of the composite film is increased with the stretching of the composite film. Compared to carbon nanotube-based ecoflex elastomer composite film, the graphene-based ecoflex composite film yields a large current–voltage signal owing to the excellent thermoelectric performance of graphene. The large current–voltage signal indicates that the thermal gradient between human skin and the ambient environment can be efficiently used for the self-powered strain sensor. The picture of 2D nanomaterial-reinforced polymer composite for the ultrasensitive self-powered strain sensor system is provided in Figure 5 in ref. [191].

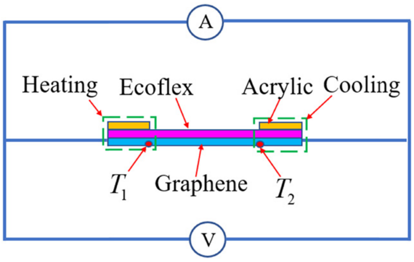

**Figure 9:** Schematic of the self-powered thermoelectric device made of graphene-based ecoflex composite film for measuring the output voltage and current under the thermal gradient ($\Delta T = T_1 - T_2$). $T_1$ denotes the temperature at the point of the heating side; $T_2$ denotes the temperature at the point of the cooling side.

A strain sensor made of 2D nanomaterial-based polymer composite is promising for use in different fields [181,192–196]. For example, structural health monitoring is a very important application of strain sensors. Infrastructures (*e.g.* dams, bridges, and buildings) are vulnerable to external loads and environmental conditions such as humidity, wind loads, and temperature variations [181]. These harsh conditions cause unpredictable and invisible structural defects in the infrastructures. As these defects develop, the infrastructures are endangered. A composite sensor can help to detect the invisible structural deterioration more efficiently and repair the structure.

# 4 Reinforcement–matrix interface

## 4.1 Influence of reinforcement–matrix interface on properties of composites

The interfacial interaction between the reinforcement and matrix has a significant influence on the mechanical properties [197–199], thermal conductivity [154], thermal stability [200], and other aspects of composites [201,202]. It is reported that an abrupt temperature drop occurs across the interface between graphene and PMMA [154], indicating inefficient thermal transport across the reinforcement–matrix interface. This is mainly due to the interfacial thermal resistance between graphene and PMMA. Furthermore, the weak interfacial interaction between 2D nanomaterials and polymer materials leads to defects and mismatches at the reinforcement–matrix interface. The defects and mismatches act as the phonon scattering [33]. As a result, the thermal conductivity of polymer composites is significantly decreased [155,156]. In addition to defects at the interface, graphene could contain Stone-Wales defects that are similar to those found in CNTs. In a previous study, it was shown that any two defects could interact between them when the CNT is loaded in tension or torsion, although the significance of the interaction diminishes with separation distance [203,204]. How the defects in graphene interact among themselves when the graphene is loaded in tension or torsion and how these interaction mechanisms affect the interaction of the graphene with the polymer matrix at the interface are still not well understood. It is reported that stress transfer between graphene and polymer materials under tension is reduced due to the deterioration of the reinforcement–matrix interface [205]. As a result, the load-carrying capacity of reinforcement (*i.e.* graphene) with high mechanical properties cannot be used fully.

The interfacial interaction between reinforcement and polymer materials also has a significant influence on the glass transition temperature of polymer composites. Due to the weak interfacial interaction between BNNS and polymer materials, the motion of polymer chains in the polymer composites cannot be effectively restricted. The loosened polymer chains lead to a reduction in the glass transition temperature of the polymer composites. As a result, the thermal stability of the composites is reduced [200]. While BNNS shows excellent thermal stability, the interface between BNNS and polymer composite can be deteriorated due to thermal-induced deformation. It is reported that the thermal-induced deformation of BNNS is irreversible at elevated temperatures [206]. This irreversible deformation of BNNS is due to the mismatch of thermal expansion between BNNS and substrate materials. As a result, the irreversible deformation of BNNS in interfacial sliding at the interface between BNNS and substrate materials. The interfacial sliding at the interface between BNNS and substrate materials inevitably reduces the reinforcing efficiency of BNNS in the mechanical properties of BNNS-based polymer composite.

## 4.2 Improvement of the reinforcement–matrix interface

As the reinforcement–matrix interface governs the mechanical, thermal, and electrical properties of polymer composites, it is necessary to enhance the interfacial matching and strength between 2D nanomaterials and polymer materials [207]. This interfacial interaction is closely related to the adhesion energy between the materials [150], which is contributed by weak nonbonded interactions such as the van der Waals interaction and electrostatic interaction. To improve the interfacial adhesion energy between 2D nanomaterials and polymer materials, one approach is to add functional groups onto the surface of 2D nanomaterials. Due to the functionalization of 2D nanomaterials, there are robust hydrogen bonds forming between 2D nanomaterials and polymer materials. Functionalization on the surface of 2D nanomaterials can be divided into two types, which are physical functionalization and chemical functionalization. The physical functionalization on the surface graphene and BNNS is not very common because the foreign materials have a weak nonbonded interaction with graphene and BNNS [208]. However, the foreign materials have a robust covalently bonded interaction with nanomaterials (*e.g.* nanotubes and nanosheets). These surface modification on nanotubes and nanosheets yields significant improvement in the physical properties of polymer composites [107,209,210]. Table 4 presents the improvement of functionalized 2D nanomaterials in the properties of polymer composites. For example, functionalized graphene causes a large restriction on the mobility of PMMA chains. As a result, the glass transition temperature of PMMA is increased. In addition, Young's modulus and tensile strength of functionalized graphene-reinforced PMMA are increased by 80 and 20%, respectively [54]. Furthermore, the functionalization of graphene shows significant improvement in viscosity [176], thermal conductivity [211], and sensitivity to mechanical motion of polymer composites [56]. These improvements are beneficial for the application of polymer composites reinforced with graphene in practice. The functionalization on the surface of BNNS is different from that on the surface of graphene because of the partial charges on the boron and nitrogen atoms. Specifically, the positively charged boron sites are reactive to nucleophilic groups (*e.g.* hydroxyl groups and amino groups), while the negatively charged nitrogen sites are attractable by electrophilic ones (*e.g.* hydrogen) [107]. With the functionalization on the surface of BNNS, the mechanical properties of the composite can be significantly increased. It is reported that an addition of 0.1% weight fraction of BNNS functionalized by hydroxyl groups increases the elastic modulus of the composite by 186% [212].

**Table 4:** Improvement of functionalized 2D nanomaterials in the properties of polymer composites

| Reinforcement | Content (wt%) | Matrix | Improvement in properties of composites |
|---|---|---|---|
| GO | 0.05 | PMMA | Glass temperature is increased by 30°C [54]<br>Young's modulus is increased by 80% [54]<br>Tensile strength is increased by 20% [54] |
| | 0.5 | PUB | Thermal conductivity is increased by 62% [211] |
| Oleylamine-BNNS | 0.1 | PVDF | Young's modulus is increased by 823% [57]<br>Tensile strength is increased by 343% [57] |
| | 4 | PVDF | The sensitivity of the sensor is increased by 10% [57] |
| Cetrimonium bromide-$MoS_2$ nanosheet | 3 | PS | Flammability is reduced by 20% [114]<br>Storage modulus is increased by 84% [213] |

In contrast, an addition of the same amount of pristine BNNS increases the elastic modulus of the composite by 20% [212]. While the surfaces of graphene and BNNS are covalently functionalized by hydroxyl, carboxyl, *etc.*, to improve the interface between graphene (or BNNS) and polymer, it is hard to modify the surface of $MoS_2$ nanosheet by chemical functionalization. To modify the surface of $MoS_2$ nanosheet, the physical functionalization can be adopted. The physical functionalization on the surface of $MoS_2$ nanosheet makes $MoS_2$ nanosheet dispersed well in organic solvents and aqueous solution. Hence, the functionalization of $MoS_2$ nanosheet shows excellent reinforcing efficiency in thermal stability and fire resistance of $MoS_2$ nanosheet-reinforced polymer composites [213]. Specifically, the addition of 3% weight fraction of $MoS_2$ nanosheet functionalized by cetrimonium bromide in polymer reduces the flammability of polymer by 20% compared with the pure polymer. Besides, the storage modulus of polymer material is increased by 84% with the addition of 3 wt% cetrimonium bromide functionalized $MoS_2$ nanosheet. The functional groups on the surface of 2D nanomaterials form robust hydrogen bonds with polymer chains. Thus, the adhesion energy between 2D nanomaterials and polymer materials is increased. In addition, these functional groups give a wrinkled structure to 2D nanomaterials, which allows mechanical interlocking with the polymer chains and improves the interfacial interaction between the reinforcement and the matrix [56,214].

# 5 Prospects

## 5.1 Hybridization of 2D nanomaterials

The application of 2D nanomaterials overcomes a lot of challenges in engineering. 2D nanomaterials show diverse characteristics and have diverse applications in engineering, as discussed in Section 3. However, one of the characteristics of the 2D nanomaterial contradicts another characteristic. For example, graphene is one of the widely used 2D nanomaterials with high thermal conductivity [114]. Hence, graphene is an attractive additive to thermal management materials. However, the nature of the electrical conductivity of graphene restricts the application of thermal manage materials containing graphene in electronics because the electronics are required to be electrically insulating to avoid short circuits. Besides, BNNS exhibits high thermal conductivity and good electrical insulation [114]. However, BNNS is hard to be dispersed in polymer materials due to its hydrophobicity and agglomeration, which reduces the thermal conductivity of BNNS-reinforced polymer composites. To make the perfect 2D nanomaterials for fulfilling the demand of thermal management materials in electronics, it is proposed to hybridize different types of 2D nanomaterials so that the shorting comings of the individual 2D nanomaterial can be overcome and the advantage of the individual 2D nanomaterial can be maintained. Specifically, the hybridized graphene/BNNS shows good solubility and dispersion, and high thermal conductivity [215]. Concurrently, the presence of BNNS hinders the electron transmission between graphene [216]. As a result, the hybridized graphene/BNNS exhibit high electrical insulation and thermal conductivity.

## 5.2 Flash synthesis of 2D nanomaterials

2D nanomaterials synthesized by top-down approach consume a large amount of solvents and energy to exfoliate from bulk materials (*e.g.* bulk graphite and hexagonal boron nitride), while the bottom-down approach yields a small amount of 2D nanomaterials and takes a lot of time [153]. Flash Joule heating is a promising method to synthesize 2D nanomaterials. This method can turn the solid waste containing prerequisite elements (*e.g.* carbon and silicon) to flash 2D nanomaterials [218–220]. For example, the solid waste containing the carbon element like rubber tires is compressed between two electrodes in a ceramic tube without requiring the furnace or solvent. The carbon source in the solid waste is turned to flash graphene by heating to 3,000 K in 100 ms during the high voltage electric discharge from a capacitor [217]. This synthesis needs no furnace, no solvent, or no purification process, which is a sustainable, environmentally friendly, and straightforward approach. Currently, this flash synthesis is widely used in producing graphene. With the development of the flash synthesis, it envisions to be used to synthesize other types of 2D nanomaterials in the future.

## 5.3 Integration of exfoliation and functionalization of 2D nanomaterials

It is discussed in Section 4 that the functionalization (*i.e.* modification) of 2D nanomaterials improves the interfacial interaction between 2D nanomaterials and polymer materials, which significantly improves the mechanical properties, thermal conductivity, viscosity, and fire retardance of 2D nanomaterial-reinforced polymer composites. In the existing literature, the exfoliation and functionalization of 2D nanomaterials are performed individually, as discussed in Secs. 2 and 4. To simplify the preparation of functionalized 2D nanomaterials, the exfoliation and functionalization of 2D nanomaterials can be performed simultaneously [107]. It is reported that the ultrasonication-based exfoliation method is used to prepare BNNS. The boron–nitrogen bonds are broken under ultrasonication. As a result, the hydroxyl group is formed on the boron sites in water [221]. Besides, in the electrochemical exfoliation, the degree of functionalization of graphene can be controlled by tuning the electrochemical exfoliation of graphene, which can control the number of defects on the surface of graphene [222].

## 5.4 Promising applications

With the development of technologies in aviation and aerospace, interplanetary travel can be realized in the future. However, space radiation (*e.g.* thermal neutron radiation) is certain to cause damage to spacecraft made of lightweight polymer composites [223]. It will be necessary to integrate radiation shielding material into polymer composites to improve the radiological tolerance of spacecraft. Polymer composites will be required to have superior load-carrying capacity and resistance to thermal and radiation attacks [224]. However, polymer materials possess low glass transmission temperature and radiation shielding capacity, indicating that spacecraft made of ordinary polymer composite will not be able to resist thermal and radiation attacks. 2D nanomaterials that exhibit multifunctional properties (*e.g.* high mechanical properties and thermal resistance) are promising in terms of improving the performance of polymer composites in the space environment. For example, the mechanical properties [55,223,225], thermal resistance [55], and shielding capacity [223,225] of polymer materials can be improved by adding BNNS. With the addition of BNNS to polymer materials, neutron radiation can be effectively shielded against, owing to the existence of $^{10}$B atoms in BNNS. $^{10}$B means boron-10, which is a stable isotope of boron with a mass number of 10. The $^{10}$B atoms have a high thermal neutron capture cross section. As a result, the neutrons can be absorbed by and react with the $^{10}$B atoms, producing free electrons [226]. This reaction transforms thermal neutron radiation into free electrons. Hence, the attack of thermal neutron radiation on spacecraft is expected to be reduced by 2D nanomaterial-reinforced polymer composites.

2D nanomaterials can also be used in nanomedical engineering (*e.g.* wound dressings, tissue engineering materials, and bioelectronic devices) [227]. With the development of nanobiotechnology, polymeric nanosheets with tens-of-nanometer thickness are fabricated. The polymeric nanosheets exhibit tunable flexibility, molecular permeability, and free-standing characteristic without being restricted by the substrates. These features make polymeric nanosheets attractive to be used to regenerate and maintain tissues and organs. It is reported that polymeric nanosheets are used to repair tissue defects, which reduces the inflammatory response or postsurgical tissue adhesion [228]. Besides, 2D nanomaterial-based polymer composite is used in bone tissue engineering. These types of artificial tissues lead to fast tissue regeneration [229]. The incorporation of 2D nanomaterials in biocomposites significantly improves the mechanical supporting capacity and biocompatibility of bone tissue and promotes cell adhesion and osteoblast differentiation [229,230]. Using the artificial tissues made of 2D nanomaterial-based biocomposite overcomes the problems in traditional bone grafting techniques (including autograft, allograft, and xenograft [231]), such as donor site pain, inflammation, graft rejection, hematoma formation, and pathogen transmission [232]. In the future, it is expected that 2D nanomaterial-based biocomposites can be used to fabricate implantable electronic devices and to connect to the living tissues for monitoring health status or providing health care.

# 6 Conclusion

The synthesis and properties of typical 2D nanomaterials, applications of polymer composites reinforced with 2D nanomaterials, and the prospects of 2D nanomaterials and polymer composites have been reviewed in this article, which is summarized as follows:

1) The mature synthesis strategies, including top-down and bottom-up strategies, yield high-quality and scalable-production 2D nanomaterials. The typical three types of 2D nanomaterials (*i.e.* graphene, BNNS, and $MoS_2$ nanosheet) exhibit higher tensile strength and Young's modulus than the traditional materials such as fibers. At the same time, these three types of 2D nanomaterials show unique characteristics. Graphene shows larger tensile strength and Young's modulus than BNNS and $MoS_2$ nanosheet, but BNNS has large thermal conductivity and low electrical conductivity. Hence, BNNS is a good candidate for improving the thermal dissipation of electronic systems. While $MoS_2$ nanosheet shows lower mechanical properties and thermal conductivity than graphene and BNNS, $MoS_2$ nanosheet is a good additive for developing strain sensors because its tunable bandgap value can effectively couple the electrical conductivity and mechanical properties.

2) Due to the properties and uniqueness of typical 2D nanomaterials, including graphene, BNNS, and $MoS_2$ nanosheet, it has been shown to be beneficial to adapt 2D nanomaterials to develop advanced polymer composites with improved structural performance, thermal dissipation of electronic systems, capability for 3D printing, and sensitivity of strain sensor.

3) The reinforcement–matrix interaction in polymer composites is of interest in terms of stress transfer and thermal transport, which significantly influences the performance and application of polymer composites reinforced with 2D nanomaterials. In terms of improving the interfacial interaction between 2D nanomaterials and polymer materials, the functionalization of 2D nanomaterials is effective in increasing the adhesion energy between the reinforcement and matrix owing to the formation of hydrogen bonds at the reinforcement–matrix interface.

4) With the development of 2D nanomaterials, it is expected that different types of 2D nanomaterials will be used to enhance the radiation shielding capacity of polymer materials in the fields of aviation and aerospace. Besides, it is expected that 2D nanomaterials can be used to repair tissue defects, promote bone tissue regeneration, and fabricate implantable electronic devices for providing health monitoring and health care in nanomedical engineering.

**Funding information**: The authors are grateful for the support from the Research Grants Council (RGC) of the Hong Kong Special Administrative Region, China (Project No. CityU 11207617), and the support from Shenzhen Science and Technology Innovation Committee under the grant JCYJ20170818103206501.

**Author contributions:** All authors have accepted responsibility for the entire content of this manuscript and approved its submission.

**Conflict of interest:** David Hui, who is the co-author of this article, is a current Editorial Board member of *Nanotechnology Reviews*. This fact did not affect the peer-review process. The authors declare no other conflict of interest.

# References

[1] Domun N, Hadavinia H, Zhang T, Sainsbury T, Liaghat GH, Vahid S. Improving the fracture toughness and the strength of epoxy using nanomaterials-a review of the current status. Nanoscale. 2015;7(23):10294–329.

[2] Lau D, Jian W, Yu Z, Hui D. Nano-engineering of construction materials using molecular dynamics simulations: prospects and challenges. Compos Pt B-Eng. 2018;143:282–91.

[3] Huang C, Qian X, Yang R. Thermal conductivity of polymers and polymer nanocomposites. Mat Sci Eng R. 2018;132:1–22.

[4] Hu K, Kulkarni DD, Choi I, Tsukruk VV. Graphene-polymer nanocomposites for structural and functional applications. Prog Polym Sci. 2014;39(11):1934–72.

[5] Srivastava VK, Gries T, Veit D, Quadflieg T, Mohr B, Kolloch M. Effect of nanomaterial on mode I and mode II interlaminar fracture toughness of woven carbon fabric reinforced polymer composites. Eng Fract Mech. 2017;180:73–86.

[6] Qin R, Zhou A, Yu Z, Wang Q, Lau D. Role of carbon nanotube in reinforcing cementitious materials: an experimental and coarse-grained molecular dynamics study. Cem Concr Res. 2021;147:106517.

[7] Bhat A, Budholiya S, Aravind Raj S, Sultan MTH, Hui D, Md Shah AU, et al. Review on nanocomposites based on aerospace applications. Nanotechnol Rev. 2021;10(1):237–53.

[8] Wang J, Cheng Q, Lin L, Chen L, Jiang L. Understanding the relationship of performance with nanofiller content in the biomimetic layered nanocomposites. Nanoscale. 2013;5(14):6356–62.

[9] Wang D, Zhang X, Zha J-W, Zhao J, Dang Z-M, Hu G-H. Dielectric properties of reduced graphene oxide/polypropylene composites with ultralow percolation threshold. Polymer. 2013;54(7):1916–22.

[10] Ramdani N, editor. Polymer nanocomposites for advanced engineering and military applications. Hershey: IGI Global; 2019.

[11] Abreu I, Ferreira DP, Fangueiro R. Versatile graphene-based fibrous systems for military applications. AVT-304. 2019.

[12] Bhattacharjee S, Joshi R, Chughtai AA, Macintyre CR. Graphene modified multifunctional personal protective clothing. Adv Mater Interfaces. 2019;6(21):1900622.

[13] Robbins JR, Ding JL, Gupta YM. Load spreading and penetration resistance of layered structures-a numerical study. Int J Impact Eng. 2004;30(6):593–615.

[14] Stankovich S, Dikin DA, Dommett GHB, Kohlhaas KM, Zimney EJ, Stach EA, et al. Graphene-based composite materials. Nature. 2006;442(7100):282–6.

[15] Wu S, Peng S, Wang CH. Multifunctional polymer nanocomposites reinforced by aligned carbon nanomaterials. Polymers. 2018;10(5):542.

[16] Kuilla T, Bhadra S, Yao D, Kim NH, Bose S, Lee JH. Recent advances in graphene based polymer composites. Prog Polym Sci. 2010;35(11):1350–75.

[17] Sun X, Sun H, Li H, Peng H. Developing polymer composite materials: carbon nanotubes or graphene? Adv Mater. 2013;25(37):5153–76.

[18] Nie F, Jian W, Lau D. An atomistic study on the thermomechanical properties of graphene and functionalized graphene sheets modified asphalt. Carbon. 2021;182:615–27.

[19] Naveen J, Jawaid M, Goh KL, Reddy DM, Muthukumar C, Loganathan TM, et al. Advancement in graphene-based materials and their nacre inspired composites for armour applications-a review. Nanomaterials. 2021;11(5):1239.

[20] Zhang Y, Ma J, Wei N, Yang J, Pei Q-X. Recent progress in the development of thermal interface materials: a review. Phys Chem Chem Phys. 2021;23(2):753–76.

[21] Li Y, Wang S, Wang Q, Xing M. A comparison study on mechanical properties of polymer composites reinforced by carbon nanotubes and graphene sheet. Compos Pt B-Eng. 2018;133:35–41.

[22] Jing C, Liu W, Hao H, Wang H, Meng F, Lau D. Regenerated and rotation-induced cellulose-wrapped oriented CNT fibers for wearable multifunctional sensors. Nanoscale. 2020;12(30):16305–14.

[23] Jian W, Lau D. Understanding the effect of functionalization in CNT-epoxy nanocomposite from molecular level. Compos Sci Technol. 2020;191:108076.

[24] Jian W, Lau D. Creep performance of CNT-based nanocomposites: a parametric study. Carbon. 2019;153:745–56.

[25] Gao Z, Zhang P, Guo J, Wang K. Bonding behavior of concrete matrix and alkali-activated mortar incorporating nano-$SiO_2$ and polyvinyl alcohol fiber: theoretical analysis and prediction model. Ceram Int. 2021;47(22):31638–49.

[26] Wang K, Zhang P, Guo J, Gao Z. Single and synergistic enhancement on durability of geopolymer mortar by polyvinyl alcohol fiber and nano-$SiO_2$. J Mater Res Technol. 2021;15:1801–14.

[27] Zhang P, Gao Z, Wang J, Wang K. Numerical modeling of rebar-matrix bond behaviors of nano-SiO2 and PVA fiber reinforced geopolymer composites. Ceram Int. 2021;47(8):11727–37.

[28] Scotti R, Conzatti L, D'Arienzo M, Di Credico B, Giannini L, Hanel T, et al. Shape controlled spherical (0D) and rod-like (1D) silica nanoparticles in silica/styrene butadiene rubber nanocomposites: role of the particle morphology on the filler reinforcing effect. Polymer. 2014;55(6):1497–506.

[29] Zhu M, Li J, Chen J, Song H, Zhang H. Improving thermal conductivity of epoxy resin by filling boron nitride nanomaterials: a molecular dynamics investigation. Comput Mater Sci. 2019;164:108–15.

[30] Chen C, Xie Y, Wang J, Lan Y, Wei X, Zhang Z. Enhancing high field dielectric properties of polymer films by wrapping a thin layer of self-assembled boron nitride film. Appl Surf Sci. 2021;535:147737.

[31] Guerra V, Wan C, McNally T. Thermal conductivity of 2D nanostructured boron nitride (BN) and its composites with polymers. Prog Mater Sci. 2019;100:170–86.

[32] Hu J, Huang Y, Zeng X, Li Q, Ren L, Sun R, et al. Polymer composite with enhanced thermal conductivity and mechanical strength through orientation manipulating of BN. Compos Sci Technol. 2018;160:127–37.

[33] Rasul MG, Kiziltas A, Arfaei B, Shahbazian-Yassar R. 2D boron nitride nanosheets for polymer composite materials. npj 2D Mater Appl. 2021;5(1):56.

[34] Veca LM, Lu F, Meziani MJ, Cao L, Zhang P, Qi G, et al. Polymer functionalization and solubilization of carbon nanosheets. Chem Commun (Cambridge, U K). 2009;18:2565–7.

[35] Zhi C, Bando Y, Tang C, Kuwahara H, Golberg D. Large-scale fabrication of boron nitride nanosheets and their utilization in polymeric composites with improved thermal and mechanical properties. Adv Mater. 2009;21(28):2889–93.

[36] Pang Y, Yang J, Curtis TE, Luo S, Huang D, Feng Z, et al. Exfoliated graphene leads to exceptional mechanical properties of polymer composite films. ACS Nano. 2019;13(2):1097–106.

[37] Wang X, Pakdel A, Zhang J, Weng Q, Zhai T, Zhi C, et al. Large-surface-area BN nanosheets and their utilization in polymeric composites with improved thermal and dielectric properties. Nanoscale Res Lett. 2012;7(1):662.

[38] Yu S, Wu X, Wang Y, Guo X, Tong L. 2D materials for optical modulation: challenges and opportunities. Adv Mater. 2017;29(14):1606128.

[39] Popa D, Sun Z, Torrisi F, Hasan T, Wang F, Ferrari AC. Sub 200 fs pulse generation from a graphene mode-locked fiber laser. Appl Phys Lett. 2010;97(20):203106.

[40] Koo J, Park J, Lee J, Jhon YM, Lee JH. Femtosecond harmonic mode-locking of a fiber laser at 3.27 GHz using a bulk-like, $MoSe_2$-based saturable absorber. Opt Express. 2016;24(10):10575–89.

[41] Cui X, Ding P, Zhuang N, Shi L, Song N, Tang S. Thermal conductive and mechanical properties of polymeric composites based on solution-exfoliated boron nitride and graphene nanosheets: a morphology-promoted synergistic effect. ACS Appl Mater Interfaces. 2015;7(34):19068–75.

[42] Wang F, Zeng X, Yao Y, Sun R, Xu J, Wong C-P. Silver nanoparticle-deposited boron nitride nanosheets as fillers for polymeric composites with high thermal conductivity. Sci Rep. 2016;6(1):19394.

[43] Shao L, Shi L, Li X, Song N, Ding P. Synergistic effect of BN and graphene nanosheets in 3D framework on the enhancement of thermal conductive properties of polymeric composites. Compos Sci Technol. 2016;135:83–91.

[44] Jia Q, Huang X, Wang G, Diao J, Jiang P. $MoS_2$ nanosheet superstructures based polymer composites for high-dielectric and electrical energy storage applications. J Phys Chem C. 2016;120(19):10206–14.

[45] Qin H, Deng C, Lu S, Yang Y, Guan G, Liu Z, et al. Enhanced mechanical property, thermal and electrical conductivity of natural rubber/graphene nanosheets nanocomposites. Polym Compos. 2020;41(4):1299–309.

[46] Li J, Gan L, Liu Y, Mateti S, Lei W, Chen Y, et al. Boron nitride nanosheets reinforced waterborne polyurethane coatings for improving corrosion resistance and antifriction properties. Eur Polym J. 2018;104:57–63.

[47] Rajabi M, Rashed GR, Zaarei D. Assessment of graphene oxide/epoxy nanocomposite as corrosion resistance coating on carbon steel. Corros Eng, Sci Technol. 2015;50(7):509–16.

[48] He J, Liu S, Li Y, Zeng S, Qi Y, Cui L, et al. Fabrication of boron nitride nanosheet/polymer composites with tunable thermal insulating properties. New J Chem. 2019;43(12):4878–85.

[49] Sato K, Ijuin A, Hotta Y. Thermal conductivity enhancement of alumina/polyamide composites via interfacial modification. Ceram Int. 2015;41(8):10314–8.

[50] Gowda A, Esler D, Tonapi S, Nagarkar K, Srihari K. Voids in thermal interface material layers and their effect on thermal performance. Proceedings of 6th Electronics Packaging Technology Conference (EPTC 2004) (IEEE Cat. No.04EX971); 2004. p. 41–6

[51] Morishita T, Okamoto H. Facile exfoliation and noncovalent superacid functionalization of boron nitride nanosheets and their use for highly thermally conductive and electrically insulating polymer nanocomposites. ACS Appl Mater Interfaces. 2016;8(40):27064–73.

[52] Fang M, Wang K, Lu H, Yang Y, Nutt S. Covalent polymer functionalization of graphene nanosheets and mechanical properties of composites. J Mater Chem. 2009;19(38):7098–105.

[53] Romasanta LJ, Hernández M, López-Manchado MA, Verdejo R. Functionalised graphene sheets as effective high dielectric constant fillers. Nanoscale Res Lett. 2011;6(1):508.

[54] Ramanathan T, Abdala AA, Stankovich S, Dikin DA, Herrera-Alonso M, Piner RD, et al. Functionalized graphene sheets for polymer nanocomposites. Nat Nanotechnol. 2008;3(6):327–31.

[55] Liang G, Sun G, Bi J, Wang W, Yang X, Li Y. Mechanical and dielectric properties of functionalized boron nitride nanosheets/silicon nitride composites. Ceram Int. 2021;47(2):2058–67.

[56] Cai D, Song M. Recent advance in functionalized graphene/polymer nanocomposites. J Mater Chem. 2010;20(37):7906–15.

[57] Sekkarapatti Ramasamy M, Rahaman A, Kim B. Influence of oleylamine-functionalized boron nitride nanosheets on the crystalline phases, mechanical and piezoelectric properties of electrospun PVDF nanofibers. Compos Sci Technol. 2021;203:108570.

[58] Tang L, Li X, Ji R, Teng KS, Tai G, Ye J, et al. Bottom-up synthesis of large-scale graphene oxide nanosheets. J Mater Chem. 2012;22(12):5676–83.

[59] Hoshiko K, Kambe T, Sakamoto R, Takada K, Nishihara H. Fabrication of dense and multilayered films of a nickel bis (dithiolene) nanosheet by means of the Langmuir-Schäfer method. Chem Lett. 2013;43(2):252–3.

[60] Kambe T, Sakamoto R, Hoshiko K, Takada K, Miyachi M, Ryu J-H, et al. π-Conjugated nickel bis(dithiolene) complex nanosheet. J Am Chem Soc. 2013;135(7):2462–5.

[61] Sakamoto R, Hoshiko K, Liu Q, Yagi T, Nagayama T, Kusaka S, et al. A photofunctional bottom-up bis(dipyrrinato)zinc(II) complex nanosheet. Nat Commun. 2015;6(1):6713.

[62] Ji X, Kong N, Wang J, Li W, Xiao Y, Gan ST, et al. A novel top-down synthesis of ultrathin 2d boron nanosheets for multimodal imaging-guided cancer therapy. Adv Mater. 2018;30(36):1803031.

[63] Cheong JY, Jung J-W, Kim C, Kim I-D. Scalable top-down synthesis of functional carbon nanosheets by aronia fruit powder for Li $^+$ and K $^+$ storage. Electrochim Acta. 2021;377:138068.

[64] Lee J, Noh S, Pham ND, Shim JH. Top-down synthesis of S-doped graphene nanosheets by electrochemical exfoliation of graphite: Metal-free bifunctional catalysts for oxygen reduction and evolution reactions. Electrochim Acta. 2019;313:1–9.

[65] Al-Dulaimi N, Lewis EA, Lewis DJ, Howell SK, Haigh SJ, O'Brien P. Sequential bottom-up and top-down processing for the synthesis of transition metal dichalcogenide nanosheets: the case of rhenium disulfide ($ReS_2$). Chem Commun (Cambridge, U K). 2016;52(50):7878–81.

[66] Zhang C, Tan J, Pan Y, Cai X, Zou X, Cheng H-M, et al. Mass production of 2D materials by intermediate-assisted grinding exfoliation. Natl Sci Rev. 2020;7(2):324–32.

[67] Le T-H, Oh Y, Kim H, Yoon H. Exfoliation of 2D materials for energy and environmental applications. Chem Eur J. 2020;26(29):6360–401.

[68] Ren W, Cheng H-M. The global growth of graphene. Nat Nanotechnol. 2014;9(10):726–30.

[69] Biccai S, Barwich S, Boland D, Harvey A, Hanlon D, McEvoy N, et al. Exfoliation of 2D materials by high shear mixing. 2D Mater. 2018;6(1):015008.

[70] Paton KR, Varrla E, Backes C, Smith RJ, Khan U, O'Neill A, et al. Scalable production of large quantities of defect-free few-layer graphene by shear exfoliation in liquids. Nat Mater. 2014;13(6):624–30.

[71] Huo C, Yan Z, Song X, Zeng H. 2D materials via liquid exfoliation: a review on fabrication and applications. Sci Bull. 2015;60(23):1994–2008.

[72] Sun Z, Yan Z, Yao J, Beitler E, Zhu Y, Tour JM. Growth of graphene from solid carbon sources. Nature. 2010;468(7323):549–52.

[73] Nageswaran VMVG. Review-2D layered metal organic framework nanosheets as an emerging platform for electrochemical sensing. J Electrochem Soc. 2020;167(13):136502.

[74] Tour JM. Top-down versus bottom-up fabrication of graphene-based electronics. Chem Mater. 2014;26(1):163–71.

[75] Brent JR, Savjani N, O'Brien P. Synthetic approaches to two-dimensional transition metal dichalcogenide nanosheets. Prog Mater Sci. 2017;89:411–78.

[76] Tour JM. Molecular Electronics. Danvers: World Scientific; 2003.

[77] Peng Y, Li Y, Ban Y, Jin H, Jiao W, Liu X, et al. Metal-organic framework nanosheets as building blocks for molecular sieving membranes. Science. 2014;346(6215):1356–9.

[78] Novoselov KS, Geim AK, Morozov SV, Jiang D, Zhang Y, Dubonos SV, et al. Electric field effect in atomically thin carbon films. Science. 2004;306(5696):666.

[79] Chen J, Duan M, Chen G. Continuous mechanical exfoliation of graphene sheets via three-roll mill. J Mater Chem. 2012;22(37):19625–8.

[80] Yi M, Shen Z. A review on mechanical exfoliation for the scalable production of graphene. J Mater Chem A. 2015;3(22):11700–15.

[81] Hernandez Y, Nicolosi V, Lotya M, Blighe FM, Sun Z, De S, et al. High-yield production of graphene by liquid-phase exfoliation of graphite. Nat Nanotechnol. 2008;3(9):563–8.

[82] Ciesielski A, Samorì P. Graphene via sonication assisted liquid-phase exfoliation. Chem Soc Rev. 2014;43(1):381–98.

[83] Achee TC, Sun W, Hope JT, Quitzau SG, Sweeney CB, Shah SA, et al. High-yield scalable graphene nanosheet production from compressed graphite using electrochemical exfoliation. Sci Rep. 2018;8(1):14525.

[84] Yu P, Lowe SE, Simon GP, Zhong YL. Electrochemical exfoliation of graphite and production of functional graphene. Curr Opin Colloid Interface Sci. 2015;20(5):329–38.

[85] Abdelkader AM, Cooper AJ, Dryfe RAW, Kinloch IA. How to get between the sheets: a review of recent works on the electrochemical exfoliation of graphene materials from bulk graphite. Nanoscale. 2015;7(16):6944–56.

[86] Sinclair RC, Suter JL, Coveney PV. Micromechanical exfoliation of graphene on the atomistic scale. Phys Chem Chem Phys. 2019;21(10):5716–22.

[87] Whitener KE, Sheehan PE. Graphene synthesis. Diamond Relat Mater. 2014;46:25–34.

[88] Novoselov KS, Jiang D, Schedin F, Booth TJ, Khotkevich VV, Morozov SV, et al. Two-dimensional atomic crystals. Proc Natl Acad Sci U S A. 2005;102(30):10451.

[89] Damm C, Nacken TJ, Peukert W. Quantitative evaluation of delamination of graphite by wet media milling. Carbon. 2015;81:284–94.

[90] Del Rio-Castillo AE, Merino C, Díez-Barra E, Vázquez E. Selective suspension of single layer graphene mechanochemically exfoliated from carbon nanofibres. Nano Res. 2014;7(7):963–72.

[91] Parvez K, Wu Z-S, Li R, Liu X, Graf R, Feng X, et al. Exfoliation of graphite into graphene in aqueous solutions of inorganic salts. J Am Chem Soc. 2014;136(16):6083–91.

[92] Beck F, Junge H, Krohn H. Graphite intercalation compounds as positive electrodes in galvanic cells. Electrochim Acta. 1981;26(7):799–809.

[93] Green TA, Quickenden TI. Calorimetric studies of highly loaded deuterides and hydrides of palladium. J Electroanal Chem. 1995;389(1):91–103.

[94] Li LH, Chen Y. Atomically thin boron nitride: unique properties and applications. Adv Funct Mater. 2016;26(16):2594–608.

[95] Pacilé D, Meyer JC, Girit ÇÖ, Zettl A. The two-dimensional phase of boron nitride: Few-atomic-layer sheets and suspended membranes. Appl Phys Lett. 2008;92(13):133107.

[96] Li LH, Chen Y, Behan G, Zhang H, Petravic M, Glushenkov AM. Large-scale mechanical peeling of boron nitride nanosheets by low-energy ball milling. J Mater Chem. 2011;21(32):11862–6.

[97] Agrawal A, Yi G-C. Chapter Two-Sample pretreatment with graphene materials. In: Hussain CM, editor. Comprehensive analytical chemistry. Amsterdam: Elsevier; 2020. p. 21–47

[98] Al-Sherbini A-S, Bakr M, Ghoneim I, Saad M. Exfoliation of graphene sheets via high energy wet milling of graphite in 2-ethylhexanol and kerosene. J Adv Res. 2017;8(3):209–15.

[99] Zhang K, Feng Y, Wang F, Yang Z, Wang J. Two dimensional hexagonal boron nitride (2D-hBN): Synthesis, properties and applications. J Mater Chem C. 2017;5(46):11992–2022.

[100] Manzeli S, Ovchinnikov D, Pasquier D, Yazyev OV, Kis A. 2D transition metal dichalcogenides. Nat Rev Mater. 2017;2(8):17033.

[101] Kappera R, Voiry D, Yalcin SE, Branch B, Gupta G, Mohite AD, et al. Phase-engineered low-resistance contacts for ultrathin $MoS_2$ transistors. Nat Mater. 2014;13(12):1128–34.

[102] Huang Y, Guo J, Kang Y, Ai Y, Li CM. Two dimensional atomically thin $MoS_2$ nanosheets and their sensing applications. Nanoscale. 2015;7(46):19358–76.

[103] Joyce BA. Molecular beam epitaxy. Rep Prog Phys. 1985;48(12):1637–97.

[104] Zhan Y, Liu Z, Najmaei S, Ajayan PM, Lou J. Large-area vapor-phase growth and characterization of $MoS_2$ atomic layers on a $SiO_2$ substrate. Small. 2012;8(7):966–71.

[105] van der Zande AM, Huang PY, Chenet DA, Berkelbach TC, You Y, Lee G-H, et al. Grains and grain boundaries in highly crystalline monolayer molybdenum disulphide. Nat Mater. 2013;12(6):554–61.

[106] Najmaei S, Liu Z, Zhou W, Zou X, Shi G, Lei S, et al. Vapour phase growth and grain boundary structure of molybdenum disulphide atomic layers. Nat Mater. 2013;12(8):754–9.

[107] Weng Q, Wang X, Wang X, Bando Y, Golberg D. Functionalized hexagonal boron nitride nanomaterials: emerging properties and applications. Chem Soc Rev. 2016;45(14):3989–4012.

[108] Tsuji Y, Kitamura Y, Someya M, Takano T, Yaginuma M, Nakanishi K, et al. Adhesion of epoxy resin with hexagonal boron nitride and graphite. ACS Omega. 2019;4(3):4491–504.

[109] Qu W, Bagchi S, Chen X, Chew HB, Ke C. Bending and interlayer shear moduli of ultrathin boron nitride nanosheet. J Phys D: Appl Phys. 2019;52(46):465301.

[110] Chen X, Yi C, Ke C. Bending stiffness and interlayer shear modulus of few-layer graphene. Appl Phys Lett. 2015;106(10):101907.

[111] He Z, Que W. Molybdenum disulfide nanomaterials: Structures, properties, synthesis and recent progress on hydrogen evolution reaction. Appl Mater Today. 2016;3:23–56.

[112] Malkappa K, Ray SS, Kumar N. Enhanced thermo-mechanical stiffness, thermal stability, and fire retardant performance of surface-modified 2D $MoS_2$ nanosheet-reinforced polyurethane composites. Macromol Mater Eng. 2019;304(1):1800562.

[113] Manzeli S, Allain A, Ghadimi A, Kis A. Piezoresistivity and strain-induced band gap tuning in atomically thin $MoS_2$. Nano Lett. 2015;15(8):5330–5.

[114] Jiang X-F, Weng Q, Wang X-B, Li X, Zhang J, Golberg D, et al. Recent progress on fabrications and applications of boron nitride nanomaterials: a review. J Mater Sci Technol. 2015;31(6):589–98.

[115] Radisavljevic B, Radenovic A, Brivio J, Giacometti V, Kis A. Single-layer $MoS_2$ transistors. Nat Nanotechnol. 2011;6(3):147–50.

[116] Castellanos-Gomez A, Poot M, Steele GA, van der Zant HSJ, Agraït N, Rubio-Bollinger G. Elastic properties of freely suspended $MoS_2$ nanosheets. Adv Mater. 2012;24(6):772–5.

[117] Sahoo S, Gaur APS, Ahmadi M, Guinel MJF, Katiyar RS. Temperature-dependent raman studies and thermal conductivity of few-layer $MoS_2$. J Phys Chem C. 2013;117(17):9042–7.

[118] Mak KF, Lee C, Hone J, Shan J, Heinz TF. Atomically thin $MoS_2$: a new direct-gap semiconductor. Phys Rev Lett. 2010;105(13):136805.

[119] Lee C, Wei X, Kysar JW, Hone J. Measurement of the elastic properties and intrinsic strength of monolayer graphene. Science. 2008;321(5887):385.

[120] Balandin AA. Thermal properties of graphene and nanostructured carbon materials. Nat Mater. 2011;10(8):569–81.

[121] Mortazavi B, Cuniberti G. Mechanical properties of polycrystalline boron-nitride nanosheets. RSC Adv. 2014;4(37):19137–43.

[122] Colas G, Serles P, Saulot A, Filleter T. Strength measurement and rupture mechanisms of a micron thick nanocrystalline $MoS_2$ coating using AFM based micro-bending tests. J Mech Phys Solids. 2019;128:151–61.

[123] Bertolazzi S, Brivio J, Kis A. Stretching and breaking of ultrathin $MoS_2$. ACS Nano. 2011;5(12):9703–9.

[124] Vadukumpully S, Paul J, Mahanta N, Valiyaveettil S. Flexible conductive graphene/poly(vinyl chloride) composite thin films with high mechanical strength and thermal stability. Carbon. 2011;49(1):198–205.

[125] Bhattacharyya A, Chen S, Zhu M. Graphene reinforced ultra high molecular weight polyethylene with improved tensile strength and creep resistance properties. Express Polym Lett. 2014;8(2):74–84.

[126] Bao C, Guo Y, Song L, Hu Y. Poly(vinyl alcohol) nanocomposites based on graphene and graphite oxide: a comparative investigation of property and mechanism. J Mater Chem. 2011;21(36):13942–50.

[127] Zhang J, Lei W, Chen J, Liu D, Tang B, Li J, et al. Enhancing the thermal and mechanical properties of polyvinyl alcohol (PVA) with boron nitride nanosheets and cellulose nanocrystals. Polymer. 2018;148:101–8.

[128] O'Neill A, Khan U, Coleman JN. Preparation of high concentration dispersions of exfoliated $MoS_2$ with increased flake size. Chem Mater. 2012;24(12):2414–21.

[129] Lau D, Broderick K, Buehler MJ, Büyüköztürk O. A robust nanoscale experimental quantification of fracture energy in a bilayer material system. Proc Natl Acad Sci USA. 2014;111(33):11990.

[130] Wang X, Xing W, Feng X, Song L, Hu Y. $MoS_2$/polymer nanocomposites: preparation, properties, and applications. Polym Rev (Philadelphia, PA, U S). 2017;57(3):440–66.

[131] Peng H, Wang D, Zhang L, Li M, Liu M, Wang C, et al. Amorphous cobalt borate nanosheets grown on $MoS_2$ nanosheet for simultaneously improving the flame retardancy and mechanical properties of polyacrylonitrile composite fiber. Compos Pt B-Eng. 2020;201:108298.

[132] Feng X, Xing W, Yang H, Yuan B, Song L, Hu Y, et al. High-performance poly(ethylene oxide)/molybdenum disulfide nanocomposite films: reinforcement of properties based on the gradient interface effect. ACS Appl Mater Interfaces. 2015;7(24):13164–73.

[133] Lin Q, Qu L, Lü Q, Fang C. Preparation and properties of graphene oxide nanosheets/cyanate ester resin composites. Polym Test. 2013;32(2):330–7.

[134] Domun N, Kaboglu C, Paton KR, Dear JP, Liu J, Blackman BRK, et al. Ballistic impact behaviour of glass fibre reinforced polymer composite with 1D/2D nanomodified epoxy matrices. Compos Pt B-Eng. 2019;167:497–506.

[135] Liu J, Liu J, Mei J, Huang W. Investigation on manufacturing and mechanical behavior of all-composite sandwich structure with Y-shaped cores. Compos Sci Technol. 2018;159:87–102.

[136] Yu S, Yu X, Ao Y, Mei J, Jiang W, Liu J, et al. The impact resistance of composite Y-shaped cores sandwich structure. Thin-Walled Struct. 2021;169:108389.

[137] Ávila AF, Neto AS, Nascimento Junior H. Hybrid nanocomposites for mid-range ballistic protection. Int J Impact Eng. 2011;38(8):669–76.

[138] Fan Y, Xiang Y, Shen H-S, Hui D. Nonlinear low-velocity impact response of FG-GRC laminated plates resting on visco-elastic foundations. Compos Pt B-Eng. 2018;144:184–94.

[139] Liu X, Sun T, Wu Z, He H. Mode II interlaminar fracture toughness of unidirectional fiber-reinforced polymer matrix composites with synthetic boehmite nanosheets at room temperature and low temperature. J Compos Mater. 2017;52(7):945–52.

[140] Ji Z, Zhang L, Xie G, Xu W, Guo D, Luo J, et al. Mechanical and tribological properties of nanocomposites incorporated with two-dimensional materials. Friction. 2020;8(5):813–46.

[141] Cai Q, Scullion D, Gan W, Falin A, Zhang S, Watanabe K, et al. High thermal conductivity of high-quality monolayer boron nitride and its thermal expansion. Sci Adv. 2019;5(6):eaav0129.

[142] Nayfeh M. Chapter 13 – advanced and low cost energy and lighting devices. In: Nayfeh M, editor. Fundamentals and applications of nano silicon in plasmonics and fullerines. Amsterdam: Elsevier; 2018. p. 363–429.

[143] Chung DDL. Materials for thermal conduction. Appl Therm Eng. 2001;21(16):1593–605.

[144] Han Z, Fina A. Thermal conductivity of carbon nanotubes and their polymer nanocomposites: a review. Prog Polym Sci. 2011;36(7):914–44.

[145] Hong H, Jung YH, Lee JS, Jeong C, Kim JU, Lee S, et al. Anisotropic thermal conductive composite by the guided assembly of boron nitride nanosheets for flexible and stretchable electronics. Adv Funct Mater. 2019;29(37):1902575.

[146] Liu X, Zhang G, Zhang Y-W. Thermal conduction across graphene cross-linkers. J Phys Chem C. 2014;118(23):12541–7.

[147] Wang Y, Xu L, Yang Z, Xie H, Jiang P, Dai J, et al. High temperature thermal management with boron nitride nanosheets. Nanoscale. 2018;10(1):167–73.

[148] Han S, Meng Q, Qiu Z, Osman A, Cai R, Yu Y, et al. Mechanical, toughness and thermal properties of 2D material-reinforced epoxy composites. Polymer. 2019;184:121884.

[149] Zeng X, Yao Y, Gong Z, Wang F, Sun R, Xu J, et al. Ice-templated assembly strategy to construct 3D boron nitride nanosheet networks in polymer composites for thermal conductivity improvement. Small. 2015;11(46):6205–13.

[150] Shen X, Wang Z, Wu Y, Liu X, He Y-B, Kim J-K. Multilayer graphene enables higher efficiency in improving thermal conductivities of graphene/epoxy composites. Nano Lett. 2016;16(6):3585–93.
[151] Kuang Z, Chen Y, Lu Y, Liu L, Hu S, Wen S, et al. Fabrication of highly oriented hexagonal boron nitride nanosheet/elastomer nanocomposites with high thermal conductivity. Small. 2015;11(14):1655–9.
[152] Wu Y, Xue Y, Qin S, Liu D, Wang X, Hu X, et al. BN nanosheet/polymer films with highly anisotropic thermal conductivity for thermal management applications. ACS Appl Mater Interfaces. 2017;9(49):43163–70.
[153] Lu H, Liang F, Gou J. Nanopaper enabled shape-memory nanocomposite with vertically aligned nickel nanostrand: controlled synthesis and electrical actuation. Soft Matter. 2011;7(16):7416–23.
[154] Zhang L, Liu L. Polymeric self-assembled monolayers anomalously improve thermal transport across graphene/polymer interfaces. ACS Appl Mater Interfaces. 2017;9(34):28949–58.
[155] Stevens RJ, Zhigilei LV, Norris PM. Effects of temperature and disorder on thermal boundary conductance at solid-solid interfaces: nonequilibrium molecular dynamics simulations. Int J Heat Mass Transfer. 2007;50(19):3977–89.
[156] Ruan K, Guo Y, Lu C, Shi X, Ma T, Zhang Y, et al. Significant reduction of interfacial thermal resistance and phonon scattering in graphene/polyimide thermally conductive composite films for thermal management. Research. 2021;2021:8438614.
[157] Amirbeygi H, Khosravi H, Tohidlou E. Reinforcing effects of aminosilane-functionalized graphene on the tribological and mechanical behaviors of epoxy nanocomposites. J Appl Polym Sci. 2019;136(18):47410.
[158] Gao X, Yue H, Guo E, Zhang S, Yao L, Lin X, et al. Tribological properties of copper matrix composites reinforced with homogeneously dispersed graphene nanosheets. J Mater Sci Technol. 2018;34(10):1925–31.
[159] Wang H, Xie G, Zhu Z, Ying Z, Zeng Y. Enhanced tribological performance of the multi-layer graphene filled poly(vinyl chloride) composites. Compos Pt A-Appl Sci Manuf. 2014;67:268–73.
[160] Rasul MG, Kiziltas A, Bin Hoque MS, Banik A, Hopkins PE, Tan K-T, et al. Improvement of the thermal conductivity and tribological properties of polyethylene by incorporating functionalized boron nitride nanosheets. Tribol Int. 2022;165:107277.
[161] Mu L, Shi Y, Feng X, Zhu J, Lu X. The effect of thermal conductivity and friction coefficient on the contact temperature of polyimide composites: experimental and finite element simulation. Tribol Int. 2012;53:45–52.
[162] Marian M, Tremmel S, Wartzack S, Song G, Wang B, Yu J, et al. Mxene nanosheets as an emerging solid lubricant for machine elements-Towards increased energy efficiency and service life. Appl Surf Sci. 2020;523:146503.
[163] Min YJ, Kang K-H, Kim D-E. Development of polyimide films reinforced with boron nitride and boron nitride nanosheets for transparent flexible device applications. Nano Res. 2018;11(5):2366–78.
[164] Chen J, Chen B, Li J, Tong X, Zhao H, Wang L. Enhancement of mechanical and wear resistance performance in hexagonal boron nitride-reinforced epoxy nanocomposites. Polym Int. 2017;66(5):659–64.
[165] Zhang Z, Breidt C, Chang L, Haupert F, Friedrich K. Enhancement of the wear resistance of epoxy: short carbon fibre, graphite, PTFE and nano-$TiO_2$. Compos Pt A-Appl Sci Manuf. 2004;35(12):1385–92.
[166] Berman D, Erdemir A, Sumant AV. Graphene: a new emerging lubricant. Mater Today. 2014;17(1):31–42.
[167] Lee C, Li Q, Kalb W, Liu X-Z, Berger H, Carpick Robert W, et al. Frictional characteristics of atomically thin sheets. Science. 2010;328(5974):76–80.
[168] Chen Z, Liu X, Liu Y, Gunsel S, Luo J. Ultrathin $MoS_2$ Nanosheets with superior extreme pressure property as boundary lubricants. Sci Rep. 2015;5(1):12869.
[169] Huang Y, Yao Q, Qi Y, Cheng Y, Wang H, Li Q, et al. Wear evolution of monolayer graphene at the macroscale. Carbon. 2017;115:600–7.
[170] Li Z-y, Yang W-j, Wu Y-p, Wu S-b, Cai Z-B. Role of humidity in reducing the friction of graphene layers on textured surfaces. Appl Surf Sci. 2017;403:362–70.
[171] Chen Z, He X, Xiao C, Kim SH. Effect of humidity on friction and wear-A critical review. Lubricants. 2018;6(3):74.
[172] Blanco I. The use of composite materials in 3D printing. J Compos Sci. 2020;4(2):42.
[173] Wang X, Jiang M, Zhou Z, Gou J, Hui D. 3D printing of polymer matrix composites: a review and prospective. Compos Pt B-Eng. 2017;110:442–58.
[174] Huber C, Abert C, Bruckner F, Groenefeld M, Muthsam O, Schuschnigg S, et al. 3D print of polymer bonded rare-earth magnets, and 3D magnetic field scanning with an end-user 3D printer. Appl Phys Lett. 2016;109(16):162401.
[175] Melnikova R, Ehrmann A, Finsterbusch K. 3D printing of textile-based structures by Fused Deposition Modelling (FDM) with different polymer materials. IOP Conf Ser: Mater Sci Eng. 2014;62:012018.
[176] Haruna MA, Pervaiz S, Hu Z, Nourafkan E, Wen D. Improved rheology and high-temperature stability of hydrolyzed polyacrylamide using graphene oxide nanosheet. J Appl Polym Sci. 2019;136(22):47582.
[177] Hofmann M. 3D printing gets a boost and opportunities with polymer materials. ACS Macro Lett. 2014;3(4):382–6.
[178] Qian Y, Li C, Qi Y, Zhong J. 3D printing of graphene oxide composites with well controlled alignment. Carbon. 2021;171:777–84.
[179] Liu M, Chiang S-W, Chu X, Li J, Gan L, He Y, et al. Polymer composites with enhanced thermal conductivity via oriented boron nitride and alumina hybrid fillers assisted by 3-D printing. Ceram Int. 2020;46(13):20810–8.
[180] Liu J, Li W, Guo Y, Zhang H, Zhang Z. Improved thermal conductivity of thermoplastic polyurethane via aligned boron nitride platelets assisted by 3D printing. Compos Pt A-Appl Sci Manuf. 2019;120:140–6.
[181] Mehmood A, Mubarak NM, Khalid M, Walvekar R, Abdullah EC, Siddiqui MTH, et al. Graphene based nanomaterials for strain sensor application-a review. J Environ Chem Eng. 2020;8(3):103743.
[182] Laukhina E, Pfattner R, Ferreras LR, Galli S, Mas-Torrent M, Masciocchi N, et al. Ultrasensitive piezoresistive all-organic flexible thin films. Adv Mater. 2010;22(9):977–81.

[183] Bae S-H, Lee Y, Sharma BK, Lee H-J, Kim J-H, Ahn J-H. Graphene-based transparent strain sensor. Carbon. 2013;51:236–42.

[184] Tan C, Dong Z, Li Y, Zhao H, Huang X, Zhou Z, et al. A high performance wearable strain sensor with advanced thermal management for motion monitoring. Nat Commun. 2020;11(1):3530.

[185] Tran L, Kim J. A comparative study of the thermoplastic polyurethane/carbon nanotube and natural rubber/carbon nanotube composites according to their mechanical and electrical properties. Fibers Polym. 2018;19(9):1948–55.

[186] Shi C, Liu X, Chuai R. Piezoresistive sensitivity, linearity and resistance time drift of polysilicon nanofilms with different deposition temperatures. Sensors. 2009;9(2):1141–66.

[187] Conley HJ, Wang B, Ziegler JI, Haglund RF, Pantelides ST, Bolotin KI. Bandgap engineering of strained monolayer and bilayer $MoS_2$. Nano Lett. 2013;13(8):3626–30.

[188] Rana V, Gangwar P, Meena JS, Ramesh AK, Bhat KN, Das S, et al. A highly sensitive wearable flexible strain sensor based on polycrystalline $MoS_2$ thin film. Nanotechnology. 2020;31(38):385501.

[189] Boland Conor S, Khan U, Ryan G, Barwich S, Charifou R, Harvey A, et al. Sensitive electromechanical sensors using viscoelastic graphene-polymer nanocomposites. Science. 2016;354(6317):1257–60.

[190] Lu L, Yang B, Liu J. Flexible multifunctional graphite nanosheet/electrospun-polyamide 66 nanocomposite sensor for ECG, strain, temperature and gas measurements. Chem Eng J. 2020;400:125928.

[191] Zhang D, Zhang K, Wang Y, Wang Y, Yang Y. Thermoelectric effect induced electricity in stretchable graphene-polymer nanocomposites for ultrasensitive self-powered strain sensor system. Nano Energy. 2019;56:25–32.

[192] Zhu M, Du X, Liu S, Li J, Wang Z, Ono T. A review of strain sensors based on two-dimensional molybdenum disulfide. J Mater Chem C. 2021;9:9083–101.

[193] Tang X, Cheng D, Ran J, Li D, He C, Bi S, et al. Recent advances on the fabrication methods of nanocomposite yarn-based strain sensor. Nanotechnol Rev. 2021;10(1):221–36.

[194] Nurazzi NM, Abdullah N, Demon SZN, Halim NA, Azmi AFM, Knight VF, et al. The frontiers of functionalized graphene-based nanocomposites as chemical sensors. Nanotechnol Rev. 2021;10(1):330–69.

[195] Sagadevan S, Shahid MM, Yiqiang Z, Oh W-C, Soga T, Anita Lett J, et al. Functionalized graphene-based nanocomposites for smart optoelectronic applications. Nanotechnol Rev. 2021;10(1):605–35.

[196] Naghib SM, Behzad F, Rahmanian M, Zare Y, Rhee KY. A highly sensitive biosensor based on methacrylated graphene oxide-grafted polyaniline for ascorbic acid determination. Nanotechnol Rev. 2020;9(1):760–7.

[197] Chen X, Zhang L, Park C, Fay CC, Wang X, Ke C. Mechanical strength of boron nitride nanotube-polymer interfaces. Appl Phys Lett. 2015;107(25):253105.

[198] Wang XQ, Jian W, Buyukozturk O, Leung CKY, Lau D. Degradation of epoxy/glass interface in hygrothermal environment: an atomistic investigation. Compos Pt B-Eng. 2021;206:108534.

[199] Qin R, Lau D. Evaluation of the moisture effect on the material interface using multiscale modeling. Multiscale Sci Eng. 2019;1(2):108–18.

[200] Qiao R, Deng H, Putz KW, Brinson LC. Effect of particle agglomeration and interphase on the glass transition temperature of polymer nanocomposites. J Polym Sci Pol Phys. 2011;49(10):740–8.

[201] Hao H, Lau D. Evolution of interfacial structure and stress induced by interfacial lattice mismatch in layered metallic nanocomposites. Adv Theory Simul. 2018;1(8):1800047.

[202] Yaphary YL, Yu Z, Lam RHW, Hui D, Lau D. Molecular dynamics simulations on adhesion of epoxy-silica interface in salt environment. Compos Pt B-Eng. 2017;131:165–72.

[203] Huq AMA, Goh KL, Zhou ZR, Liao K. On defect interactions in axially loaded single-walled carbon nanotubes. J Appl Phys. 2008;103(5):054306.

[204] Huq AMA, Bhuiyan AK, Liao KIN, Goh KL. Defect-defect interaction in single-walled carbon nanotubes under torsional loading. Int J Mod Phys B. 2010;24(10):1215–26.

[205] Young RJ, Gong L, Kinloch IA, Riaz I, Jalil R, Novoselov KS. Strain mapping in a graphene monolayer nanocomposite. ACS Nano. 2011;5(4):3079–84.

[206] Qu W, Gou F, Ke C. Thermal-induced irreversible straining of ultrathin boron nitride nanosheets. Appl Phys Lett. 2019;114(5):051901.

[207] Li J, Chen J, Zhu M, Song H, Zhang H. Interfacial characteristics of boron nitride nanosheet/epoxy resin nanocomposites: a molecular dynamics simulation. Appl Sci. 2019;9(14):2832.

[208] Biroju RK, Giri PK. Defect enhanced efficient physical functionalization of graphene with gold nanoparticles probed by resonance raman spectroscopy. J Phys Chem C. 2014;118(25):13833–43.

[209] Lu H, Min Huang W. Synergistic effect of self-assembled carboxylic acid-functionalized carbon nanotubes and carbon fiber for improved electro-activated polymeric shape-memory nanocomposite. Appl Phys Lett. 2013;102(23):231910.

[210] Kuila T, Bose S, Mishra AK, Khanra P, Kim NH, Lee JH. Chemical functionalization of graphene and its applications. Prog Mater Sci. 2012;57(7):1061–105.

[211] Du W, Zhang Z, Su H, Lin H, Li Z. Urethane-functionalized graphene oxide for improving compatibility and thermal conductivity of waterborne polyurethane composites. Ind Eng Chem Res. 2018;57(21):7146–55.

[212] Sainsbury T, Satti A, May P, Wang Z, McGovern I, Gun'ko YK, et al. Oxygen radical functionalization of boron nitride nanosheets. J Am Chem Soc. 2012;134(45):18758–71.

[213] Zhou K, Liu J, Wen P, Hu Y, Gui Z. A noncovalent functionalization approach to improve the dispersibility and properties of polymer/$MoS_2$ composites. Appl Surf Sci. 2014;316:237–44.

[214] Shahsavari R. Intercalated hexagonal boron nitride/silicates as bilayer multifunctional ceramics. ACS Appl Mater Interfaces. 2018;10(3):2203–9.

[215] Hosseini E, Zakertabrizi M, Habibnejad Korayem A, Shahsavari R. Tunable, multifunctional ceramic composites via intercalation of fused graphene boron nitride nanosheets. ACS Appl Mater Interfaces. 2019;11(8):8635–44.

[216] Ren J, Li Q, Yan L, Jia L, Huang X, Zhao L, et al. Enhanced thermal conductivity of epoxy composites by introducing

graphene@boron nitride nanosheets hybrid nanoparticles. Mater Des. 2020;191:108663.

[217] Luong DX, Bets KV, Algozeeb WA, Stanford MG, Kittrell C, Chen W, et al. Gram-scale bottom-up flash graphene synthesis. Nature. 2020;577(7792):647–51.

[218] Barbhuiya NH, Kumar A, Singh A, Chandel MK, Arnusch CJ, Tour JM, et al. The future of flash graphene for the sustainable management of solid waste. ACS Nano. 2021;15(10):15461–70.

[219] Advincula PA, Luong DX, Chen W, Raghuraman S, Shahsavari R, Tour JM. Flash graphene from rubber waste. Carbon. 2021;178:649–56.

[220] Yan X, Sun W, Wang W, Duchesne PN, Deng X, He J, et al. solid-solid synthesis of silicon oxide nanorods. Small. 2020;16(35):2001435.

[221] Wang W, Chen SJ, Basquiroto de Souza F, Wu B, Duan WH. Exfoliation and dispersion of boron nitride nanosheets to enhance ordinary Portland cement paste. Nanoscale. 2018;10(3):1004–14.

[222] Campéon BDL, Akada M, Ahmad MS, Nishikawa Y, Gotoh K, Nishina Y. Non-destructive, uniform, and scalable electrochemical functionalization and exfoliation of graphite. Carbon. 2020;158:356–63.

[223] Harrison C, Weaver S, Bertelsen C, Burgett E, Hertel N, Grulke E. Polyethylene/boron nitride composites for space radiation shielding. J Appl Polym Sci. 2008;109(4):2529–38.

[224] Tang L, Zhang J, Tang Y, Kong J, Liu T, Gu J. Polymer matrix wave-transparent composites: a review. J Mater Sci Technol. 2021;75:225–51.

[225] Fang H, Bai S-L, Wong CP. Thermal, mechanical and dielectric properties of flexible BN foam and BN nanosheets reinforced polymer composites for electronic packaging application. Compos Pt A-Appl Sci Manuf. 2017;100:71–80.

[226] Maity A, Doan TC, Li J, Lin JY, Jiang HX. Realization of highly efficient hexagonal boron nitride neutron detectors. Appl Phys Lett. 2016;109(7):072101.

[227] Fujie T, Takeoka S. Advances in nanosheet technology towards nanomedical engineering. NanoBiotechnology. 2014;68:68.

[228] Fujie T. Development of free-standing polymer nanosheets for advanced medical and health-care applications. Polym J (Tokyo, Jpn). 2016;48(7):773–80.

[229] Adithya SP, Sidharthan DS, Abhinandan R, Balagangadharan K, Selvamurugan N. Nanosheets-incorporated bio-composites containing natural and synthetic polymers/ceramics for bone tissue engineering. Int J Biol Macromol. 2020;164:1960–72.

[230] Li X, Shan J, Zhang W, Su S, Yuwen L, Wang L. Recent advances in synthesis and biomedical applications of two-dimensional transition metal dichalcogenide nanosheets. Small. 2017;13(5):1602660.

[231] Pape HC, Evans A, Kobbe P. Autologous bone graft: properties and techniques. J Orthop Trauma. 2010;24:S36–40.

[232] Wang W, Yeung KWK. Bone grafts and biomaterials substitutes for bone defect repair: a review. Bioact Mater. 2017;2(4):224–47.